Ferrofluid irreversibility and heat transfer simulation inside a permeable space including Lorentz forces

Li, Zhixiong; Hedayat, Mohammadali; Arabkoohsar, Ahmad; Sheikholeslami, M.; Shafee, Ahmad; Ayed, Mossaad Ben; Tlili, I.; Nguyen, Truong Khang

Published in:
Physica A: Statistical Mechanics and its Applications

DOI (link to publication from Publisher):
10.1016/j.physa.2019.121492

Publication date:
2019

Document Version
Accepted author manuscript, peer reviewed version

Accepted Manuscript

Ferrofluid irreversibility and heat transfer simulation inside a permeable space including Lorentz forces

Zhixiong Li, Mohammadali Hedayat, A. Arabkoohsar, M. Sheikholeslami, Ahmad Shafee, Mossaad Ben Ayed, I. Tlili, Truong Khang Nguyen

PII: S0378-4371(19)30885-4
DOI: https://doi.org/10.1016/j.physa.2019.121492
Article number: 121492
Reference: PHYSA 121492

To appear in: *Physica A*

Received date : 7 January 2019
Revised date : 5 April 2019

Please cite this article as: Z. Li, M. Hedayat, A. Arabkoohsar et al., Ferrofluid irreversibility and heat transfer simulation inside a permeable space including Lorentz forces, *Physica A* (2019), https://doi.org/10.1016/j.physa.2019.121492

*Highlights (for review)

Highlights

- ✓ Ferrofluid exergy behavior is investigated within porous media.
- ✓ CVFEM is implemented to model MHD effect on nanofluid.
- ✓ Entropy generation augments with rise of Hartmann number.
- ✓ Bejan number has direct relationship with magnetic field.

Ferrofluid irreversibility and heat transfer simulation inside a permeable space including Lorentz forces

Zhixiong Li [a,b], Mohammadali Hedayat [c], A. Arabkoohsar [d], M. Sheikholeslami [e], Ahmad Shafee [f], Mossaad Ben Ayed [g,h], I. Tlili [i], Truong Khang Nguyen [1,j,k]

[a] School of Engineering, Ocean University of China, Qingdao 266110, China
[b] School of Mechanical, Materials, Mechatronic and Biomedical Engineering, University of Wollongong, Wollongong, NSW 2522, Australia
[c] J. Mike Walker '66 Department of Mechanical Engineering, Texas A&M University, College Station, USA
[d] Department of Energy Technology, Aalborg University, Denmark
[e] Department of Mechanical Engineering, Babol Noshirvani University of Technology, Babol, Islamic Republic of Iran
[f] Public Authority of Applied Education & Training, College of Technological Studies, Applied Science Department, Shuwaikh, Kuwait
[g] Computer Science Department, College of Science and Humanities at Alghat, Majmaah University, Al-Majmaah, 11952, Saudi Arabia
[h] Computer and Embedded System Laboratory, Sfax University, Tunisia
[i] Department of Mechanical and Industrial Engineering, College of Engineering, Majmaah University, Al-Majmaah 11952, Saudi Arabia
[j] Division of Computational Physics, Institute for Computational Science, Ton Duc Thang University, Ho Chi Minh City, Vietnam
[k] Faculty of Electrical and Electronics Engineering, Ton Duc Thang University, Ho Chi Minh City, Vietnam

Abstract

In current paper, exergy simulation of free convection is scrutinized. In current mathematical framework, uniform magnetic field is adopted. In order to save the time, single phase model has been involved for nanofluid. Trend of Darcy, Hartmann and Rayleigh numbers on Bejan number, exergy loss and Nusselt number are captured through figures. Obtained outputs have indicated the growth of Nu_{ave} with the Darcy and Rayleigh numbers. A growth of Lorenz forces reflects greater exergy loss. To get the desired outcomes for application prospective, lower Hartmann number should be selected.

Keywords: CVFEM; Exergy; Nanofluid; Heat transfer; Lorentz force.

[1] Corresponding author:
Email: nguyentruongkhang@tdtu.edu.vn (Truong Khang Nguyen)

1. Introduction

Mixing of nanoparticles in a pure carrier fluid significantly augment the thermal conductivity, consequently improve heat transfer rate which can be helpful in various industrial process. Common used coolant, like water for illustration, is about three orders magnitude lower in the heat conduction when compared with metals. Recent decades, nanofluids are utilized in numerous areas [1-9]. Rashid et al. [10] carried out the macroscopic modeling for wavy porous duct including second grade fluid. They imposed both magnetic and electric fields. Non-Newtonian flow due to Lorentz forces and imposed chemical reaction was investigated by Roy and Gorla [11]. They reported lower skin friction with rise of magnetic forces. Their outputs indicated that Schmidt number has direct relation with Sherwood number.

New modeling approach for analyzing entropy generation of nanofluid has been offered by Sheikholeslami [12]. He displayed that permeability has reverse relation with Bejan number. Third grad nanofluid movement within non stationary domain was simulated by Shah et al. [13]. They supposed that bottom wall is stretched. They incorporated thermophoresis impact on energy transportation. Impact of chemical reaction on Eyring-Powell fluid motion has been scrutinized by Hayat and Nadeem [14]. They evidenced that concentration declines with rise of reaction parameter. Thermal radiation impact on nanoparticle thermal behavior was explained by Nasir et al. [15]. They imposed MHD and reported Sherwood number to describe concentration of nanofluid. Various nanoparticles have been tested by Rehman and Nadeem [16] for nanofluid transport along stretching forces. Maximum Nusselt number has been obtained with selecting copper. Two magnetic sources' impacts on thermal treatment of ferrofluid were investigated by Muhammad et al. [17]. They demonstrated that temperature profile augments with rise of ferrohydrodynamic parameter. Prandtl fluid model formulation has been constructed by Bilal et al. [18]. They also involved thermo diffusion impacts. They concluded that Sherwood number declines with augment of Dufour number. Nanofluid layer behavior in existence of EHD has been analyzed by Moatimid and Hassan [19]. They provided instability analysis for two pure fluids. Numerical developments for thermal analysis have been presented by various researchers [20-28].

In current study, we discuss the new model for magnetic force impact on nanomaterial convection by including homogenous model for ferrofluid. Exergy analysis was examined in view of second law approach. Last equations with considering non-Darcy law was simulated via innovative approach namely CVFEM which is less employed for computations of nonlinear systems.

2. Explanation of problem and method

Consider the laminar, steady free convection of H_2O based ferrofluid in a permeable region with involving Lorentz forces. Fig. 1 describes the domain in which inner side imposed the constant heat flux. We assumed that viscous dissipation and joule heating were negligible. To add the permeability in momentum equations, Non-Darcy model was incorporated. To simplify the governing equations, pressure source terms were discarded with involving Ψ-ω formulation. CVFEM was implemented to solve the equations. This approach is very powerful due to this fact that it uses not only the advantage of FVM but also it uses the benefits of FEM for discretization [29]. To save time in simulation single phase model was employed for nanomaterial. Considering two dimensional problem leads to below equations [29]:

$$\frac{\partial v}{\partial y}+\frac{\partial u}{\partial x}=0 \qquad (1)$$

$$\left(B_y, B_x\right) = B_o\left(\sin\gamma, \cos\gamma\right), \tag{2}$$

$$\left(\rho_{nf}\right)\left(\frac{\partial u}{\partial y}v + u\frac{\partial u}{\partial x}\right) = \left[B_y v\,\sigma_{nf} B_x - B_y^2 \sigma_{nf} u + \left(\frac{\partial^2 u}{\partial y^2} + \frac{\partial^2 u}{\partial x^2}\right)\mu_{nf} - \frac{\partial P}{\partial x} - u\frac{\mu_{nf}}{K}\right],$$

$$g\left(T - T_c\right)\beta_{nf}\,\rho_{nf} - \frac{\partial P}{\partial y} + \mu_{nf}\left(\frac{\partial^2 v}{\partial y^2} + \frac{\partial^2 v}{\partial x^2}\right) - \frac{\mu_{nf}}{K}v \tag{3}$$

$$-B_x v B_x \sigma_{nf} + B_x u\,\sigma_{nf} B_y = \left(v\frac{\partial v}{\partial y} + \frac{\partial v}{\partial x}u\right)\rho_{nf},$$

$$\left(u\frac{\partial T}{\partial x} + \frac{\partial T}{\partial y}v\right) = k_{nf}\left(\frac{\partial^2 T}{\partial x^2} + \frac{\partial^2 T}{\partial y^2}\right) / \left(\rho C_p\right)_{nf} \tag{4}$$

As we mentioned, to estimate the properties of carrier fluid, homogenous model with following formulas was employed:

$$CC = (1-\phi) + \left(\rho C_p\right)_s \phi / \left(\rho C_p\right)_f,\ CC = \left(\rho C_p\right)_{nf} / \left(\rho C_p\right)_f \tag{5}$$

$$BB = \phi\left(\rho\beta\right)_s / \left(\rho\beta\right)_f + (1-\phi),\ BB = \left(\rho\beta\right)_{nf} / \left(\rho\beta\right)_f \tag{6}$$

$$\rho_s\phi + (1-\phi)\rho_f = \rho_{nf} \tag{7}$$

$$\frac{\sigma_{nf}}{\sigma_f} = 1 + \frac{3(-1+\Delta)\phi}{(2+\Delta) - (-1+\Delta)\phi},\ \sigma_s / \sigma_f = \Delta \tag{8}$$

$$kk = \left(\frac{2k_f + 2\phi kd + k_s}{2k_f - kd\,\phi + k_s}\right),\ kk = k_{nf} / k_f,\ kd = k_s - k_f \tag{9}$$

$$\mu_{nf} = e^{-0.01T}\left(-27886.4807\phi^2 + 3.1B + 4263.02\phi + 316.0629 + 0.035B^2\right) \tag{10}$$

Features of nanomaterial were portrayed in table 1. To simplify the above equations, Eq. (11) was implemented and then Eq. (12) was employed to reach last equations:

$$\psi_x = -v, v_x - u_y = -\omega, \frac{\partial \psi}{\partial y} = u, \tag{11}$$

$$(X, Y) = (x, y) L^{-1}, \Delta T = q'' L / k_f, V \alpha_f L^{-1} = v, \Theta = \frac{T - T_c}{\Delta T}, \alpha_f U L^{-1} = u, \tag{12}$$

Thus, the last equations have following forms:

$$\begin{aligned}
&\left(\frac{\partial \Theta}{\partial X}\right) \Pr Ra \left(A_2^2 \frac{A_3}{A_4^2 A_1}\right) + \Pr \left(\frac{A_2 A_5}{A_4 A_1}\right) \left(\frac{\partial^2 \Omega}{\partial Y^2} + \frac{\partial^2 \Omega}{\partial X^2}\right) \\
&+ \Pr Ha^2 \left[\frac{A_2 A_6}{A_4 A_1}\right] \left(-(\sin\gamma) \frac{\partial V}{\partial Y} (\cos\gamma) + (\cos\gamma) \frac{\partial U}{\partial X} (\sin\gamma)\right) \\
&+ \Pr Ha^2 \left[\frac{A_2 A_6}{A_4 A_1}\right] \left((\sin\gamma)^2 \frac{\partial U}{\partial Y} - (\cos\gamma)^2 \frac{\partial V}{\partial X}\right) \\
&- \left(\frac{A_5}{A_4 A_1}\right) \Omega \frac{\Pr}{Da} A_2 = U \frac{\partial \Omega}{\partial X} + \frac{\partial \Omega}{\partial Y} V
\end{aligned} \tag{13}$$

$$V \frac{\partial \Theta}{\partial Y} + U \frac{\partial \Theta}{\partial X} = \left(\frac{\partial^2 \Theta}{\partial Y^2} + \frac{\partial^2 \Theta}{\partial X^2}\right) \tag{14}$$

$$\frac{\partial^2 \Psi}{\partial Y^2} + \frac{\partial^2 \Psi}{\partial X^2} = -\Omega \tag{15}$$

Dimensionless parameters which are used above equations and boundary conditions are as follows:

$$\begin{aligned}
&Da = \frac{K}{L^2}, Ra = \beta_f g q'' L^4 / (k_f \upsilon_f \alpha_f), \\
&A_6 = \frac{\sigma_{nf}}{\sigma_f}, A_2 = \frac{(\rho C_P)_{nf}}{(\rho C_P)_f}, \\
&A_5 = \frac{\mu_{nf}}{\mu_f}, \Pr = \upsilon_f / \alpha_f, A_1 = \frac{\rho_{nf}}{\rho_f}, A_4 = \frac{k_{nf}}{k_f}, \\
&Ha = \sqrt{\sigma_f / \mu_f} B_0 L, A_3 = \frac{(\rho\beta)_{nf}}{(\rho\beta)_f}
\end{aligned} \tag{16}$$

$$\left.\frac{\partial \Theta}{\partial n}\right|_{inner} = 1.0, \left.\Psi\right|_{all} = 0.0, \left.\Theta\right|_{outer} = 0.0 \tag{17}$$

Nu_{loc} and Nu_{ave} are determined from:

$$Nu_{loc} = A_4\left(Rd\,\frac{4}{3A_4}+1\right)\frac{1}{\Theta} \tag{18}$$

$$Nu_{ave} = \frac{1}{S}\int_0^S Nu_{loc}\,ds \tag{19}$$

$S_{gen,total}$, Be and X_d were calculated according to below formulas:

$$S_{gt} = \underbrace{\frac{\mu_{nf}}{TK}\left(u^2+v^2\right)}_{S_{gen,P}} \tag{20}$$

$$+\underbrace{v^2\sigma_{nf}B_0^2T^{-2}}_{S_{gen,M}}+\underbrace{T^{-2}\left[\left(\frac{\partial T}{\partial x}\right)^2+\left(\frac{\partial T}{\partial y}\right)^2\right]k_{nf}}_{S_{gen,th}}$$

$$+\underbrace{\left[2\left(\frac{\partial u}{\partial x}\right)^2+2\left(\frac{\partial v}{\partial y}\right)^2+\left(\frac{\partial v}{\partial x}+\frac{\partial u}{\partial y}\right)^2\right]\mu_{nf}T^{-2}}_{S_{gen,f}}$$

$$Be = S_{gen,th}/S_{gt} \tag{21}$$

$$X_d = S_{gt}T_0 \tag{22}$$

3. Results and discussion

Simulations were executed to illustrate the new concept of energy and exergy treatment of convective flow of nanomaterial within a permeable region. Non Darcy and single phase models were incorporated considering Ψ-ω formulation. The governing non dimensional system has been figure out numerically by means of CVFEM. Influences of buoyancy and Lorentz forces were accounted in view of entropy analysis.

Prior to the validation and presenting outputs, the mesh sensitivity analysis has been examined. As displayed in table 2, Nu_{ave} has no changes after 3rd mesh, so this grid can guarantee a grid independent output. The computational outputs for the special case have been verified by comparisons with current outputs in existing studies [30] in table 3 and the outputs were in nice agreement. Figs. 2, 3, 4 and 5 portray various components of entropy, *Be* and X_d as well as nanomaterial hydrothermal behavior. At low values of *Da* and *Ra*, contours expounded that the isotherms forms a pack of straight lines along the boundaries which indicates conduction mode. By augmenting Rayleigh number, nanofluid transport boosts up and convection develops but it has an inverse correlation with Bejan number. Thermal plume can be progressed easily in greater values of Ra. When permeability of region augments, it improves the convection. Also, thinner boundary layer was reported as a result of augmenting Rayleigh number. Thermal boundary thickness grows when *Ha* augments. Entropy generation reinforces with augment of magnetic forces. One can perceived that nanofluid transportation enhances with rise of Darcy number. So, exergy loss declines with augment of *Da*. *Be* and X_d have inverse relation with permeability and buoyancy force. So, with augment of *Ra* and *Da*, entropy generation become weaker and as an outputs less resistance has been affected the domain. Boundary layer thickness becomes thicker for greater Hartmann number due to reduction of flow in appearance of resisting force. Beside, exergy loss has direct relation with Lorentz forces. Similar trend is reported for Bejan number.

Be, Nu_{ave}, and X_d variations were deliberated in Figs. 6, 7 and 8 for different active parameters. In addition, following formulas can be offered:

$$\begin{aligned} Nu_{ave} &= 1.11 + 0.033Da + 0.21\log(Ra) - 0.41Ha \\ &+ 0.035Da\log(Ra) - 0.22Da\,Ha - 0.13\log(Ra)Ha \end{aligned} \tag{23}$$

$$\begin{aligned} Be &= 0.95 - 8.5\times10^{-3}Da - 0.0931\log(Ra) + 0.03Ha \\ &- 5.38\times10^{-3}Da\log(Ra) + 3.25\times10^{-3}Da\,Ha + 0.019\log(Ra)Ha \end{aligned} \tag{24}$$

$$X_d = 70.64 - 1.34Da - 7.71\log(Ra) + 14.43Ha + 0.13Da\log(Ra) + 7.23Da\,Ha + 1.29\log(Ra)Ha \quad (25)$$

Temperature distribution augments with greater values of Darcy number. So, free convection proliferates with *Da*. Stronger resisting force can be obtained with rise of Ha. Thus, Nu_{ave} declines with rise of *Ha*. There are reductions in *Be* and X_d for higher values of *Da* and *Ra*.

4. Conclusions

This paper was focused on nanofluid, laminar, free convection in a porous domain including exergy analysis. Non-Darcy model and Lorentz forces impacts were incorporated. The homogeneous model was utilized to characterize the features of nanomaterial. Comparison of our outputs with previous outputs was made for various Ra and found to be in nice agreement. The outputs revealed that the exergy loss is in a direction proportion with Hartmann number. For higher values of Da, nanofluid motion enriches and consequently Nu_{ave} augments. Isotherms becomes curvy with rise of permeability

Acknowledgment: Dr. Mossaad Ben Ayed would like to thank Deanship of Scientific Research at Majmaah University for supporting this work under the Project Number No. 1440-51.

References

[1] Sivasankaran, S., A. I. Alsabery, and I. Hashim, Internal heat generation effect on transient natural convection in a nanofluid-saturated local thermal non-equilibrium porous inclined cavity, Physica A: Statistical Mechanics and its Applications 509, (2018) 275-293

[2] GHR Kefayati, NAC Sidik, Simulation of natural convection and entropy generation of non-Newtonian nanofluid in an inclined cavity using Buongiorno's mathematical model (Part II, entropy generation), Powder Technology 305 (2017) 679-703.

[3] M. Sheikholeslami, M. Jafaryar, Ahmad Shafee, Zhixiong Li, Rizwan Ul Haq, Heat transfer of nanoparticles employing innovative turbulator considering entropy generation, International Journal of Heat and Mass Transfer 136 (2019) 1233-1240

[4] S. Nadeem, Shafiq Ahmad, Noor Muhammad, Computational study of Falkner-Skan problem for a static and moving wedge Sensors and Actuators, B: Chemical (2018) 263 DOI: 10.1016/j.snb.2018.02.039

[5] Mohsen Sheikholeslami, Ahmad Arabkoohsar, Ilyas Khan, Ahmad Shafee, Zhixiong Li, Impact of Lorentz forces on Fe3O4-water ferrofluid entropy and exergy treatment within a permeable semi annulus, Journal of Cleaner Production, 221 (2019) 885-898

[6] S. Ijaz, S. Nadeem, Consequences of blood mediated nano transportation as drug agent to attenuate the atherosclerotic lesions with permeability impacts, Journal of Molecular Liquids, 262 (2018) 565-575

[7] M. Sheikholeslami, Rizwan-ul Haq, Ahmad Shafee, Zhixiong Li, Yassir G. Elaraki, I. Tlili, Heat transfer simulation of heat storage unit with nanoparticles and fins through a heat exchanger, International Journal of Heat and Mass Transfer 135 (2019) 470–478

[8] Xiaohong Su, Liancun Zheng, Xinxin Zhang, Junhong Zhang, MHD mixed convective heat transfer over a permeable stretching wedge with thermal radiation and ohmic heating, Chemical Engineering Science, 78 (2012) 1-8

[9] S. Ijaz, S. Nadeem, A biomedical solicitation examination of nanoparticles as drug agents to minimize the hemodynamics of a stenotic channel, Eur. Phys. J. Plus (2017) 132: 448. https://doi.org/10.1140/epjp/i2017-11703-6

[10] M. Rashid, Iqra Shahzadi, S. Nadeem, Corrugated walls analysis in microchannels through porous medium under Electromagnetohydrodynamic (EMHD) effects, Results in Physics 9 (2018) 171-182

[11] Nepal C. Roy, R. S. R. Gorla, Effects of radiation and magnetic field on mixed convection flow of non-Newtonian power-law fluids across a cylinder in the presence of chemical reaction, Heat and Mass Transfer, Vol. 55, No. 2, pp. 341–351 (2019). doi:10.1007/s00231-018-2413-4

[12] M. Sheikholeslami, New computational approach for exergy and entropy analysis of nanofluid under the impact of Lorentz force through a porous media, Computer Methods in Applied Mechanics and Engineering 344 (2019) 319–333

[13] Zahir Shah, Saeed Islam,Taza Gul, Ebenezer Bonyah, Altaf Khan, Three dimensional third grade nanofluid flow in a rotating system between parallel plates with Brownian motion and thermophoresis effects, Results in Phys. 10 (2018) 36–45

[14] Tanzila Hayat, S. Nadeem, Flow of 3D Eyring-Powell fluid by utilizing Cattaneo-Christov heat flux model and chemical processes over an exponentially stretching surface, Results in Physics 8 (2018) 397-403

[15] Saleem Nasir, Saeed Islam, Taza Gul, Zahir Shah, Muhammad Altaf Khan, Waris Khan, Aurang Zeb Khan, Saima Khan, Three dimensional rotating flow of MHD single wall carbon nanotubes over a stretching sheet in presence of thermal radiation, Applied Nanoscience, https://doi.org/10.1007/s13204-018-0766-0.

[16] Fiaz Ur Rehman, S. Nadeem, Heat Transfer Analysis for Three-Dimensional Stagnation-Point Flow of Water-Based Nanofluid over an Exponentially Stretching Surface, Journal of Heat Transfer (2018) 140(5) HT-17-1037; doi: 10.1115/1.4038359

[17] Noor Muhammad, Sohail Nadeem, MT Mustafa, Impact of magnetic dipole on a thermally stratified ferrofluid past a stretchable surface, Proceedings of the Institution of Mechanical Engineers, Part E: Journal of Process Mechanical Engineering (2018) https://doi.org/10.1177/0954408918759244

[18] S. Bilal, K.U. Rehman, M.Y. Malik, A. Hussain, M. Awais, Effect logs of double diffusion on MHD Prandtl nano fluid adjacent to stretching surface by way of numerical approach, Results in Physics 7 (2017) 470-479.

[19] Galal M. Moatimid and Mohamed A. Hassan, Linear Instability of Water–Oil Electrohydrodynamic Nanofluid Layers: Analytical and Numerical Study, Journal of Computational and Theoretical Nanoscience 15 (2018) 1495-1510

[20] Fengrui Sun, Yuedong Yao, Xiangfang Li, Pengliang Yu, Guanyang Ding, Ming Zou, The flow and heat transfer characteristics of superheated steam in offshore wells and analysis of superheated steam performance, Computers & Chemical Engineering, 2017, 100: 80-93.

[21] M. Sheikholeslami, M. Jafaryar, Ahmad Shafee, Zhixiong Li, Simulation of nanoparticles application for expediting melting of PCM inside a finned enclosure, Physica A: Statistical Mechanics and its Applications 523 (2019) 544–556

[22] Fiaz Ur Rehman, S. Nadeem, Rizwan Ul Haq, Heat transfer analysis for three-dimensional stagnation-point flow over an exponentially stretching surface, Chinese Journal of Physics 55 (2017) 1552-1560

[23] M. Sheikholeslami, Omid Mahian, Enhancement of PCM solidification using inorganic nanoparticles and an external magnetic field with application in energy storage systems, Journal of Cleaner Production 215 (2019) 963-977

[24] Fengrui Sun, Yuedong Yao, Xiangfang Li, Lin Zhao, Guanyang Ding, Xuejiao Zhang, The Mass and Heat Transfer Characteristics of Superheated Steam Coupled with Non-condensing Gases in Perforated Horizontal Wellbores, Journal of Petroleum Science and Engineering, 2017, 156: 460-467.

[25] M. Sheikholeslami, Rizwan-ul Haq, Ahmad Shafee, Zhixiong Li, Heat transfer behavior of Nanoparticle enhanced PCM solidification through an enclosure with V shaped fins, International Journal of Heat and Mass Transfer 130 (2019) 1322–1342

[26] Houman B. Rokni, Joshua D. Moore, Ashutosh Gupta, Mark A. McHugh, Manolis Gavaises, Entropy scaling based viscosity predictions for hydrocarbon mixtures and diesel fuels up to extreme conditions, Fuel 241 (2019) 1203-1213

[27] M. Sheikholeslami, Numerical approach for MHD Al2O3-water nanofluid transportation inside a permeable medium using innovative computer method, Computer Methods in Applied Mechanics and Engineering 344 (2019) 306–318

[28] Xiao-hong Su, Lian-cun Zheng, Xin-xin Zhang, DTM-BF method and dual solutions for unsteady MHD flow over permeable shrinking sheet with velocity slip, Applied Mathematics and Mechanics, 33 (2012) 1555–1568

[29] Mohsen Sheikholeslami, Application of Control Volume based Finite Element Method (CVFEM) for Nanofluid Flow and Heat Transfer, Elsevier, (2019), ISBN: 9780128141526

[30] G. De Vahl Davis, Natural convection of air in a square cavity, a benchmark numerical solution, Int. J. Numer. Methods Fluids 3 (1962) 249–264.

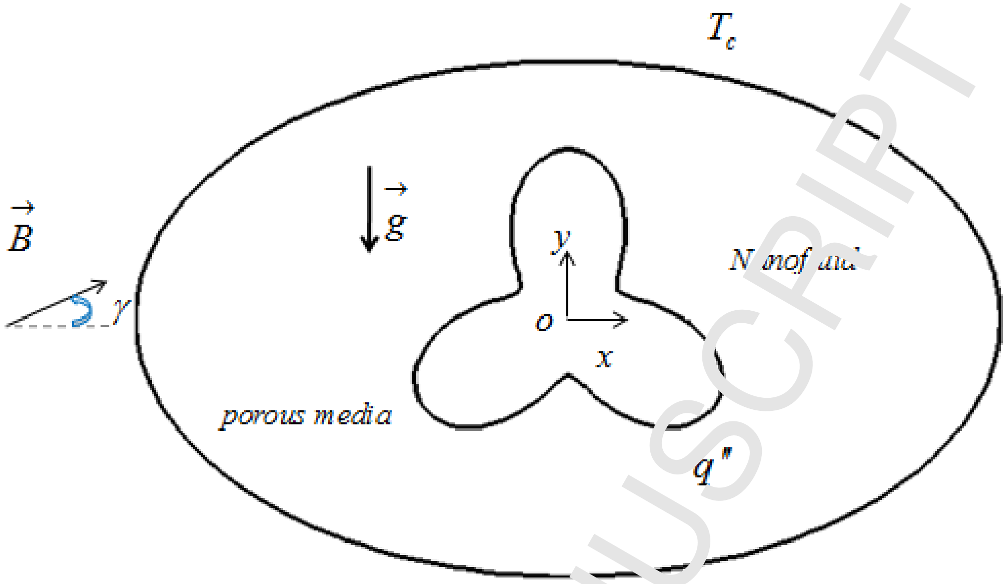

Fig. 1. Current domain with constant heat flux

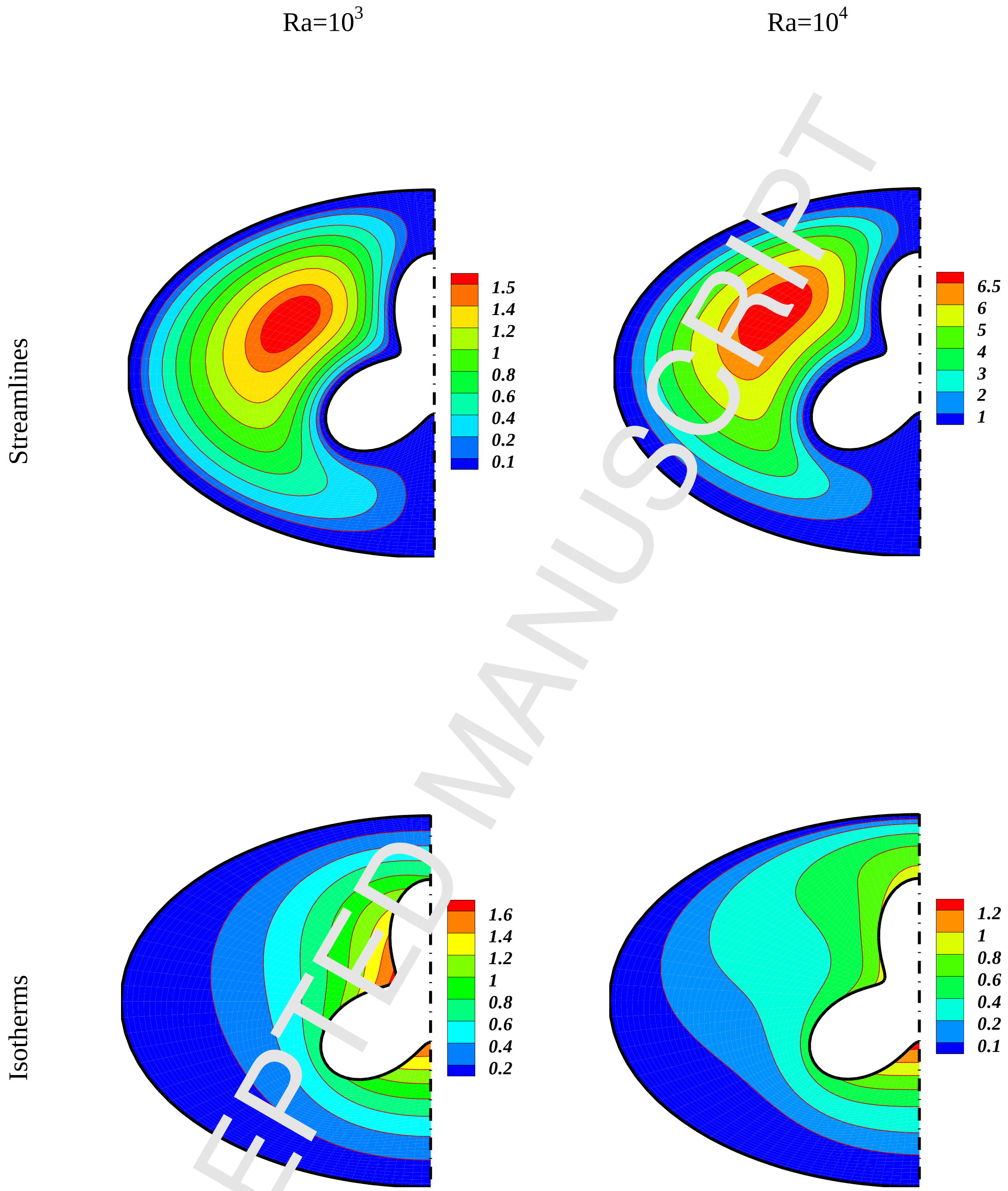

Ra=10^3
Ra=10^4
Streamlines
1.5
1.4
1.2
1
0.8
0.6
0.4
0.2
0.1
6.5
6
5
4
3
2
1
Isotherms
1.6
1.4
1.2
1
0.8
0.6
0.4
0.2
1.2
1
0.8
0.6
0.4
0.2
0.1

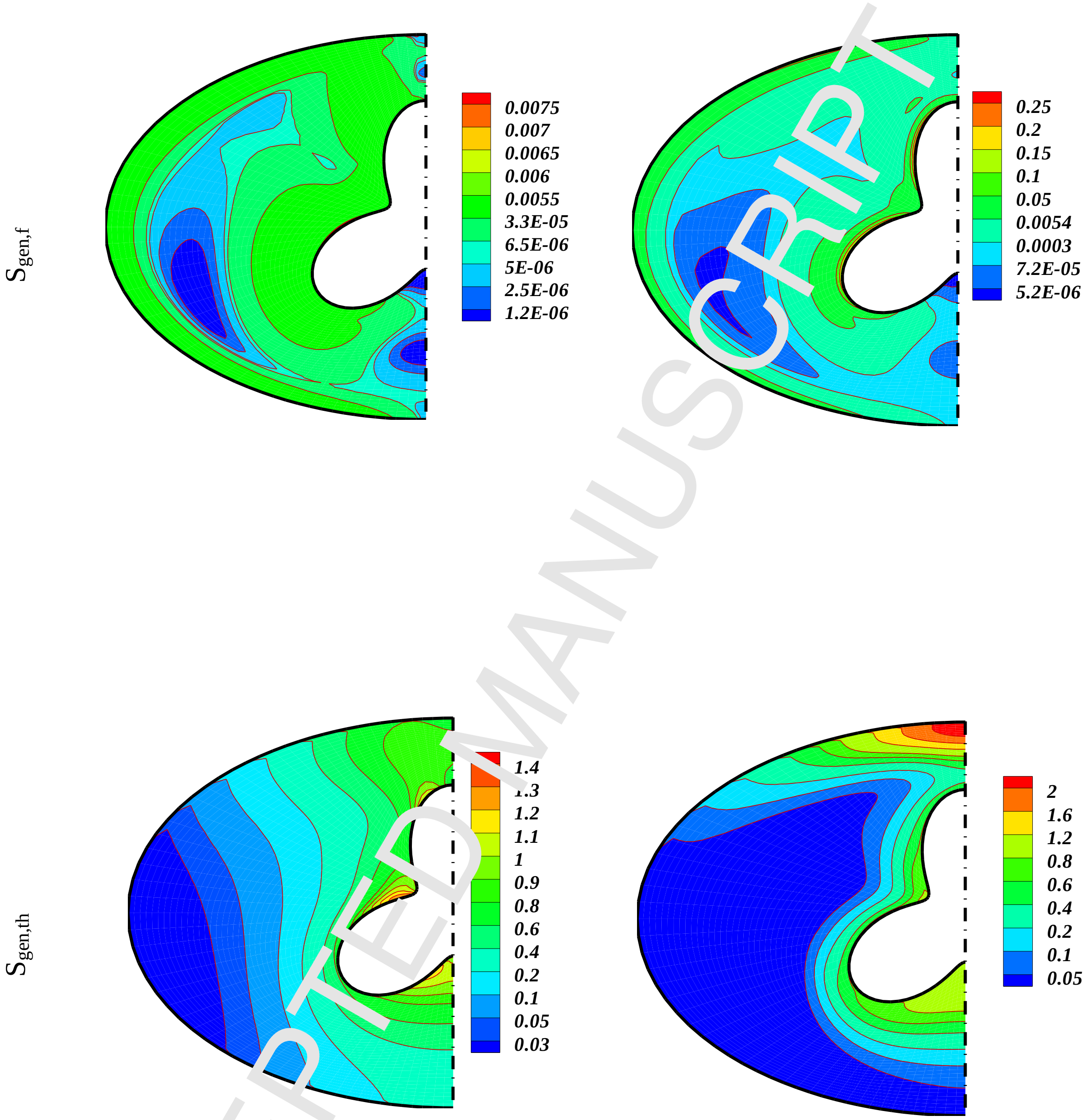
S gen,f
0.0075
0.007
0.0065
0.006
0.0055
3.3E-05
6.5E-06
5E-06
2.5E-06
1.2E-06
0.25
0.2
0.15
0.1
0.05
0.0054
0.0003
7.2E-05
5.2E-06
S gen,th
1.4
1.3
1.2
1.1
1
0.9
0.8
0.6
0.4
0.2
0.1
0.05
0.03
2
1.6
1.2
0.8
0.6
0.4
0.2
0.1
0.05

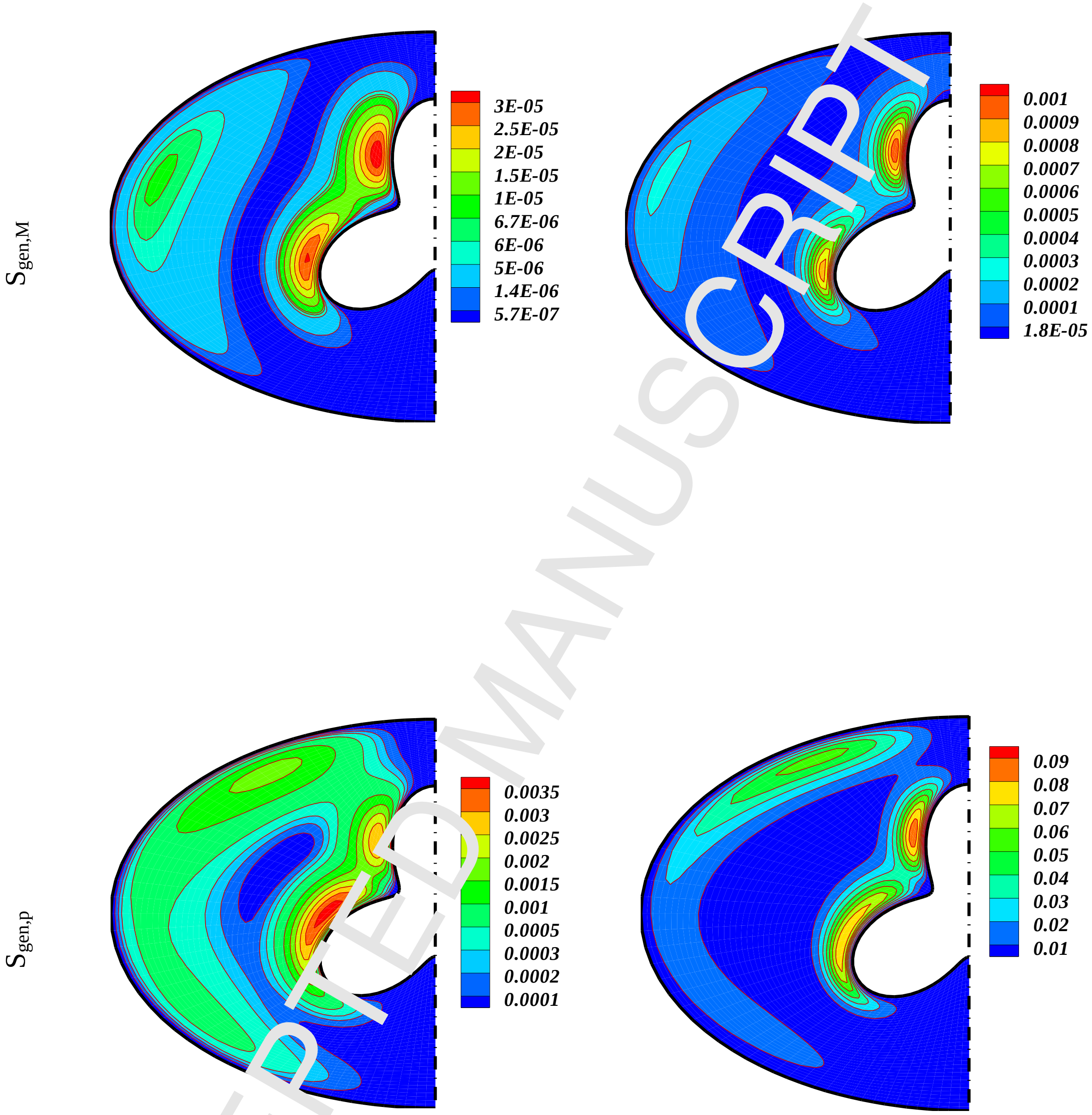
S gen,M
3E-05
2.5E-05
2E-05
1.5E-05
1E-05
6.7E-06
6E-06
5E-06
1.4E-06
5.7E-07
0.001
0.0009
0.0008
0.0007
0.0006
0.0005
0.0004
0.0003
0.0002
0.0001
1.8E-05
S gen,p
0.0035
0.003
0.0025
0.002
0.0015
0.001
0.0005
0.0003
0.0002
0.0001
0.09
0.08
0.07
0.06
0.05
0.04
0.03
0.02
0.01

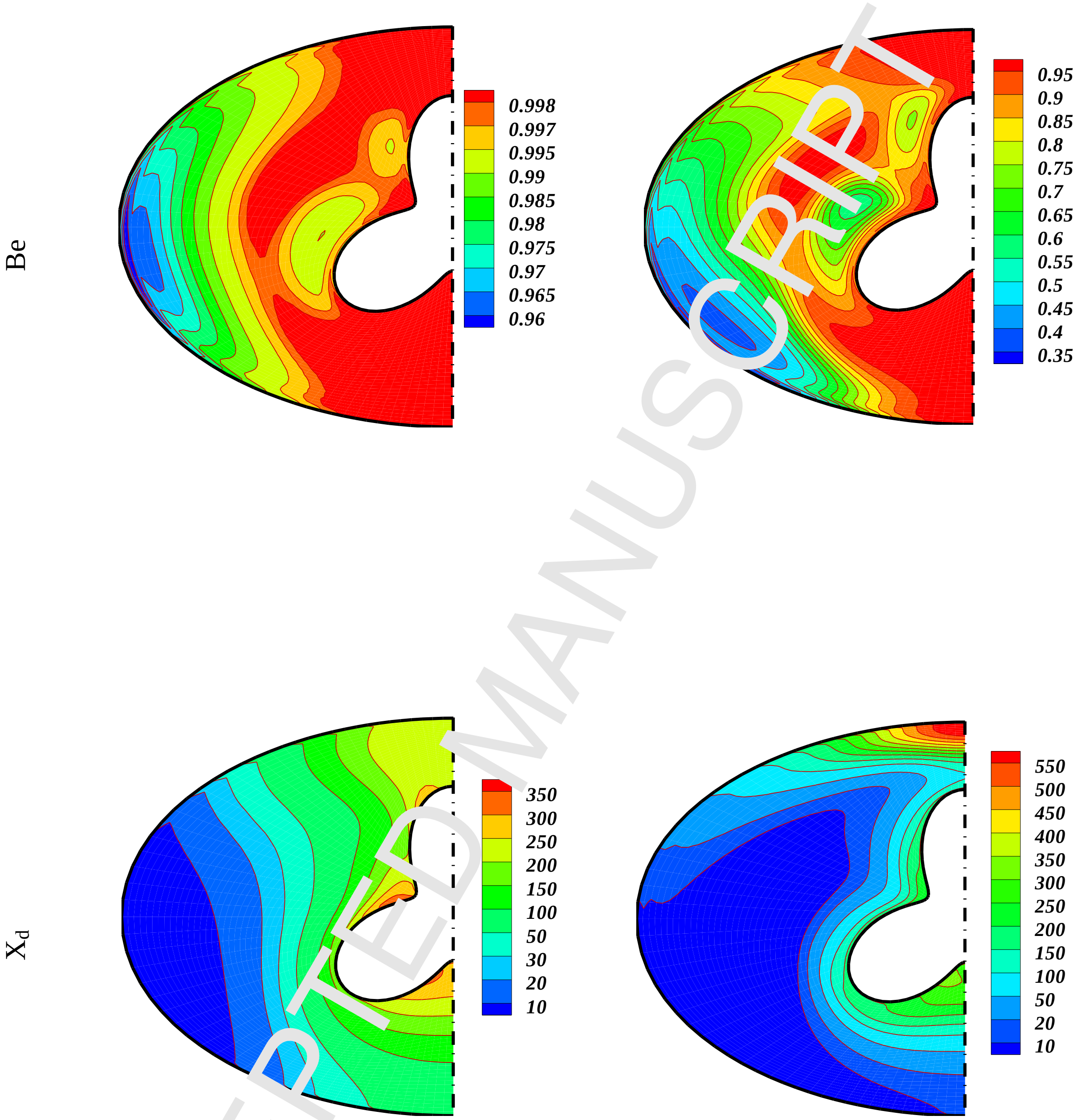

Fig. 2. Outputs for various *Ra* at $\phi = 0.04, Ha = 1, Da = 0.01$

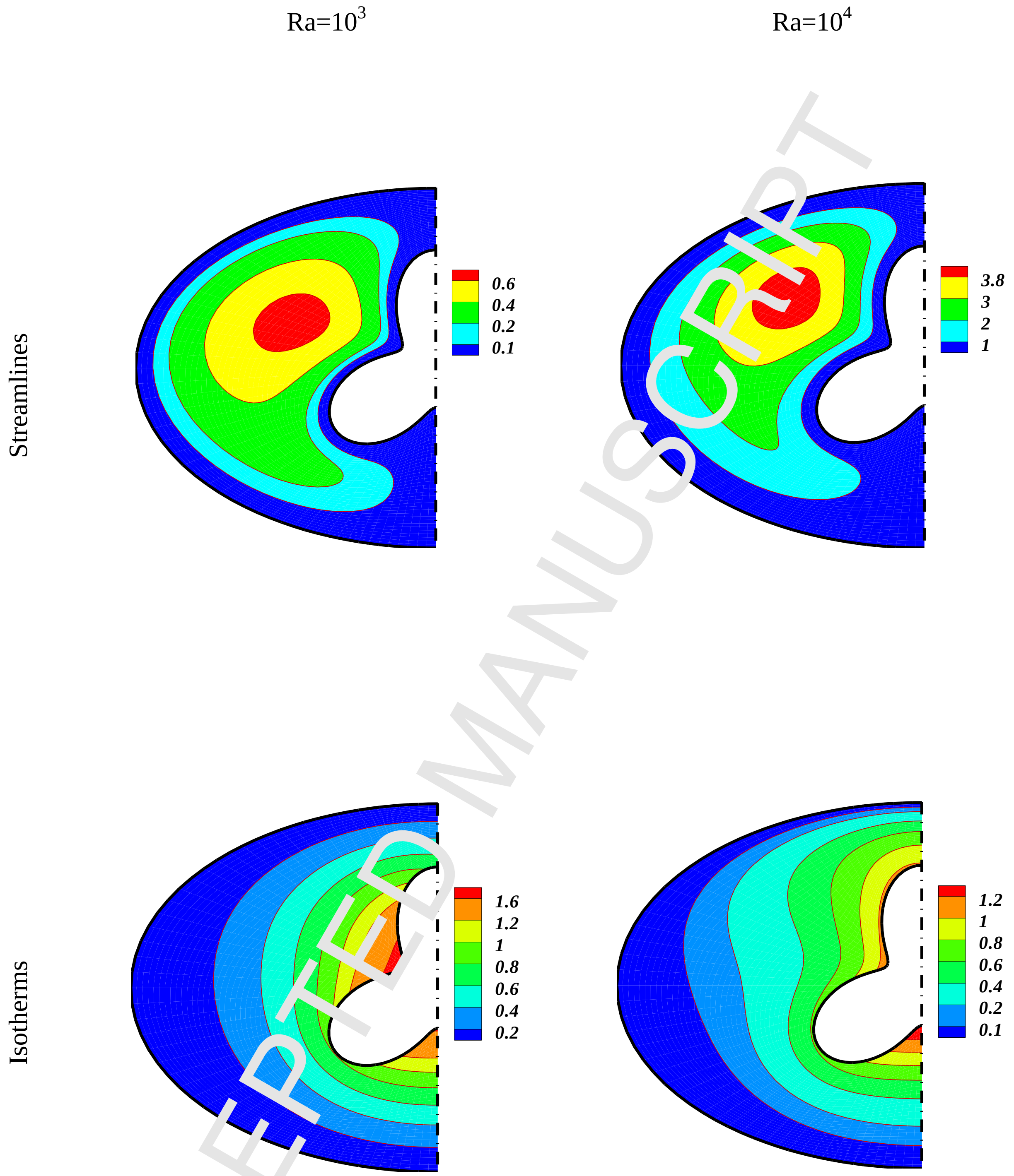
Ra=10^3
Ra=10^4
Streamlines
Isotherms
0.6
0.4
0.2
0.1
3.8
3
2
1
1.6
1.2
1
0.8
0.6
0.4
0.2
1.2
1
0.8
0.6
0.4
0.2
0.1

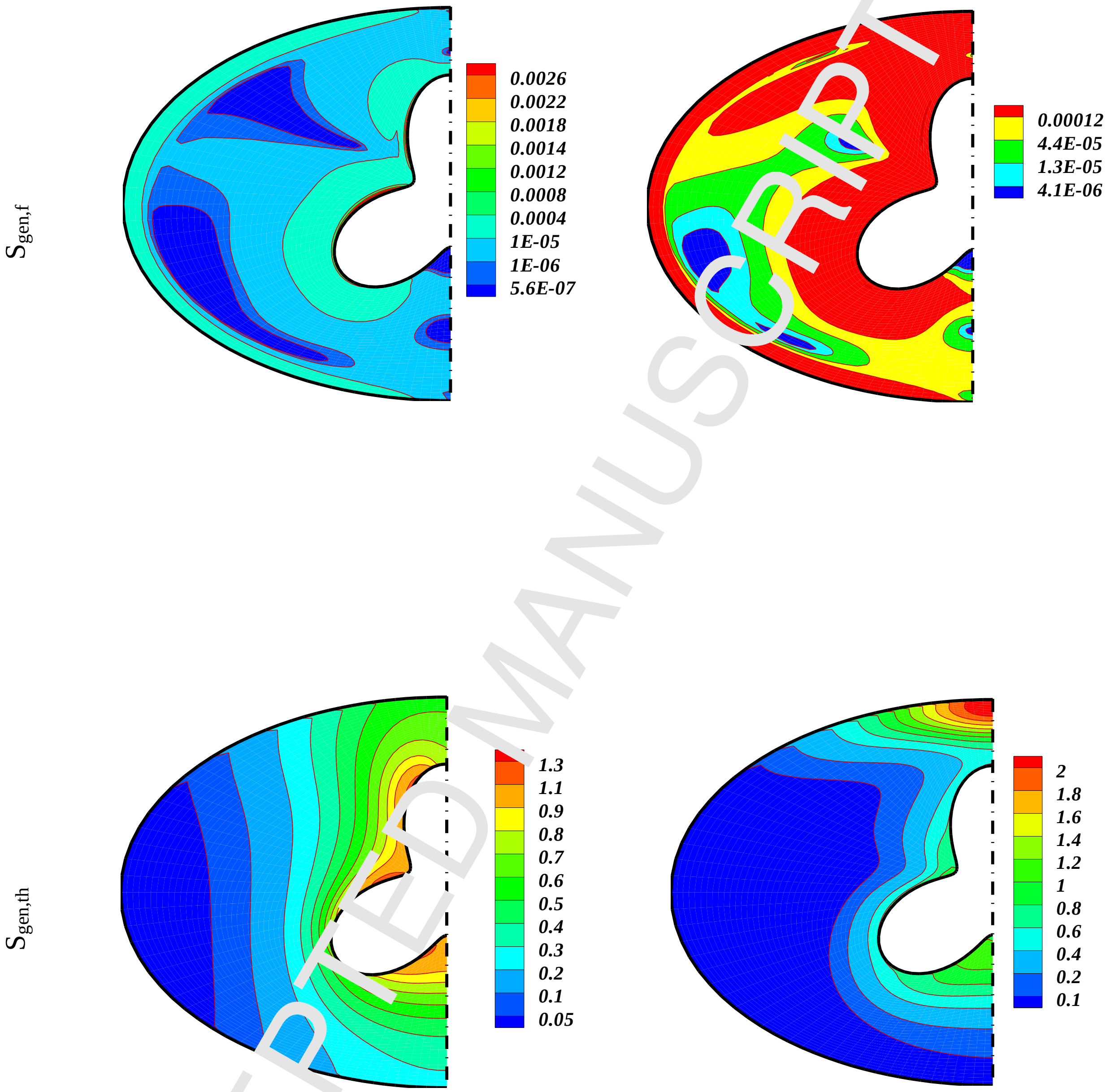

$S_{gen,f}$
0.0026
0.0022
0.0018
0.0014
0.0012
0.0008
0.0004
1E-05
1E-06
5.6E-07
0.00012
4.4E-05
1.3E-05
4.1E-06
$S_{gen,th}$
1.3
1.1
0.9
0.8
0.7
0.6
0.5
0.4
0.3
0.2
0.1
0.05
2
1.8
1.6
1.4
1.2
1
0.8
0.6
0.4
0.2
0.1

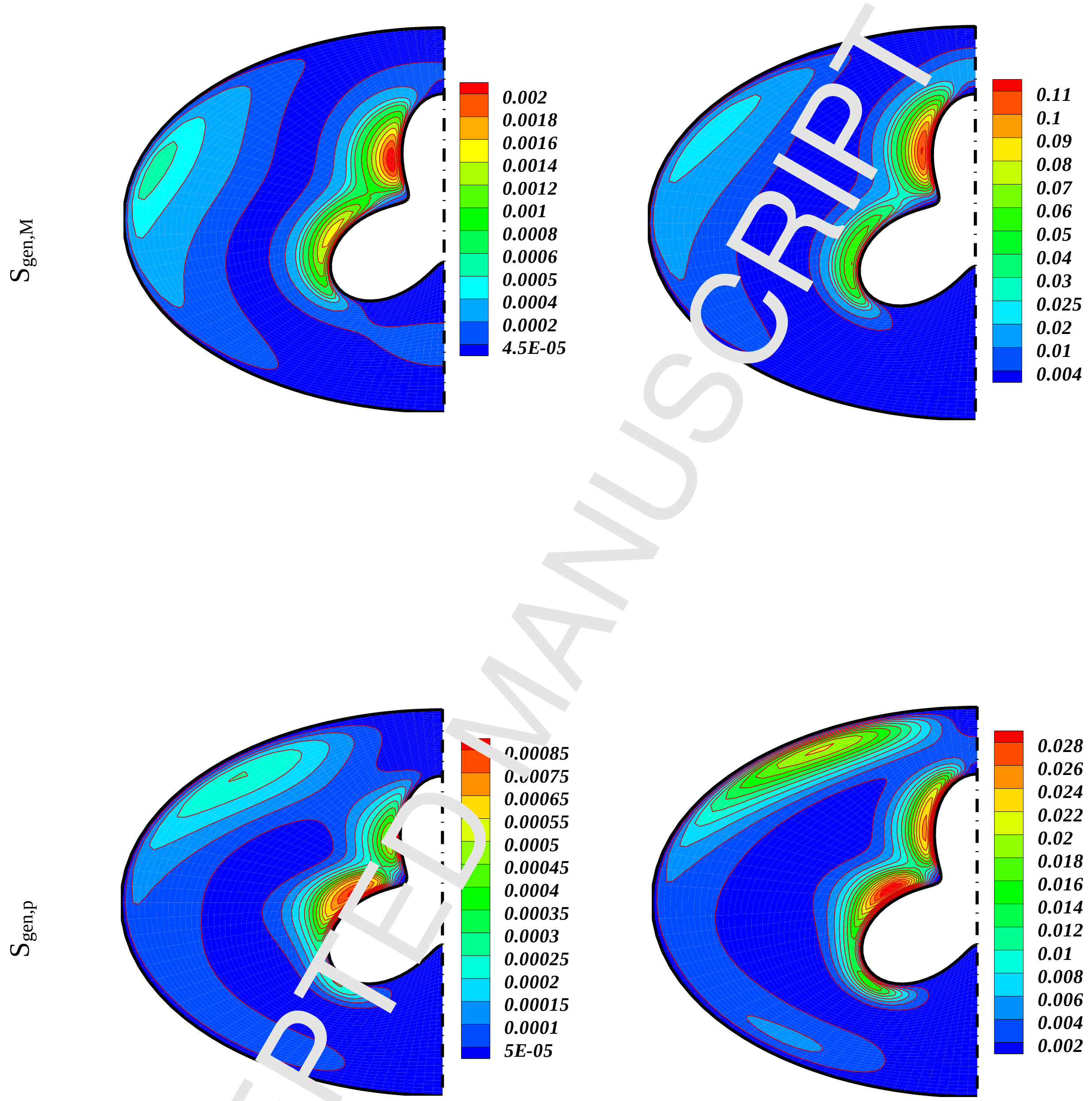

$S_{gen,M}$
0.002
0.0018
0.0016
0.0014
0.0012
0.001
0.0008
0.0006
0.0005
0.0004
0.0002
4.5E-05
0.11
0.1
0.09
0.08
0.07
0.06
0.05
0.04
0.03
0.025
0.02
0.01
0.004
$S_{gen,p}$
0.00085
0.00075
0.00065
0.00055
0.0005
0.00045
0.0004
0.00035
0.0003
0.00025
0.0002
0.00015
0.0001
5E-05
0.028
0.026
0.024
0.022
0.02
0.018
0.016
0.014
0.012
0.01
0.008
0.006
0.004
0.002

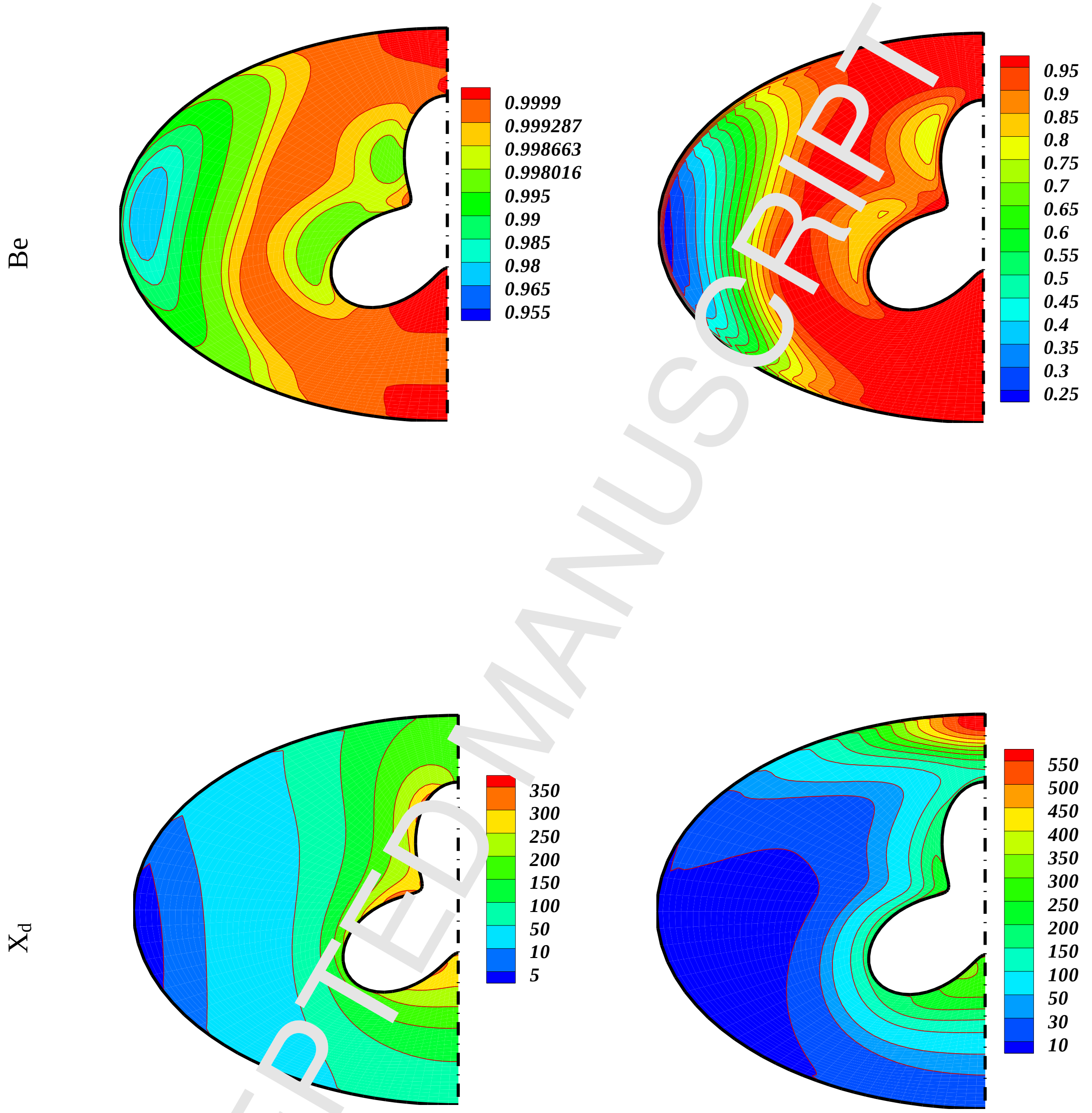

Fig. 3. Outputs for various *Ra* at $\phi = 0.04$, $Ha = 20$, $Da = 0.01$

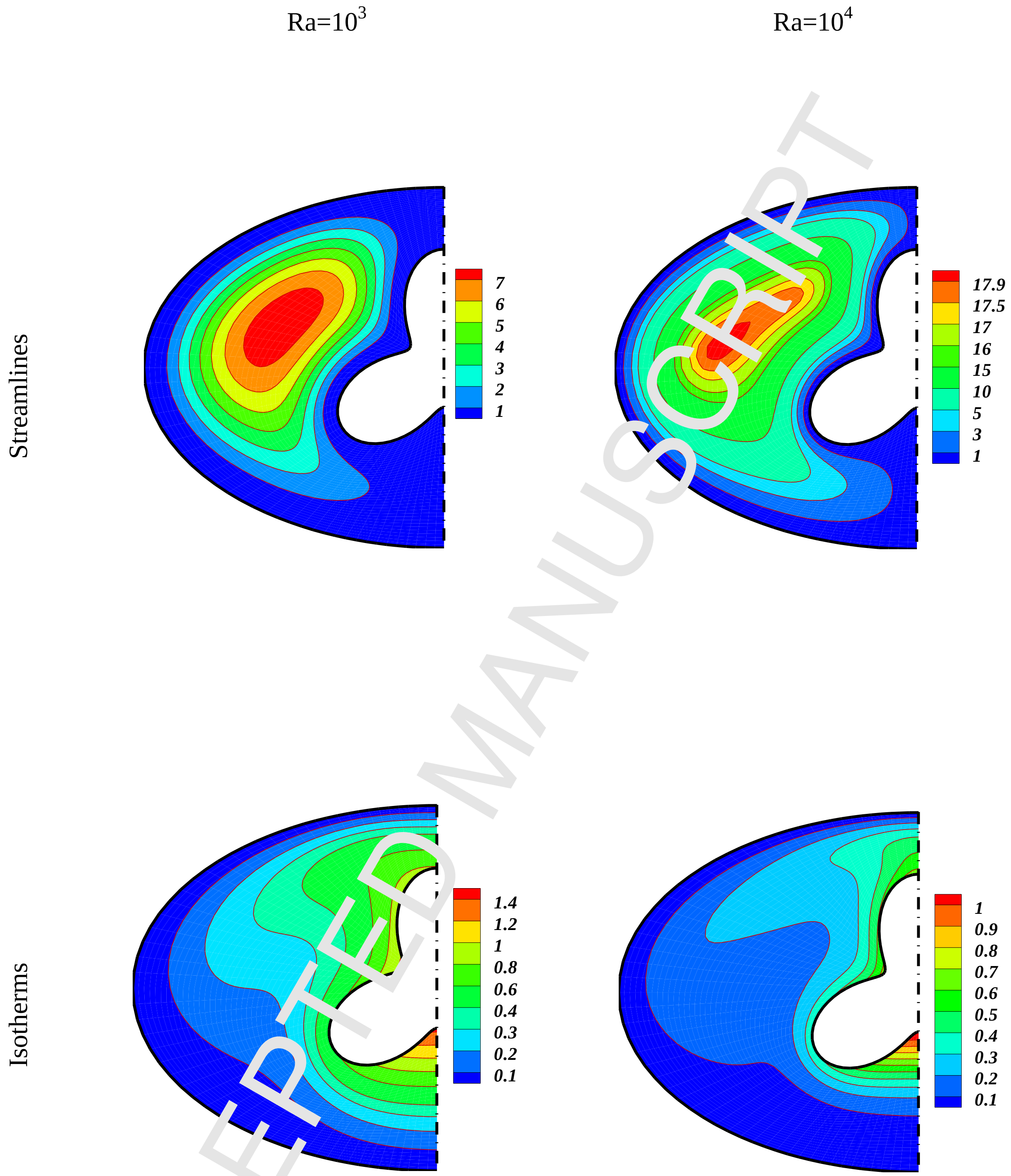

Ra=10^3
Ra=10^4
Streamlines
7
6
5
4
3
2
1
17.9
17.5
17
16
15
10
5
3
1
Isotherms
1.4
1.2
1
0.8
0.6
0.4
0.3
0.2
0.1
1
0.9
0.8
0.7
0.6
0.5
0.4
0.3
0.2
0.1

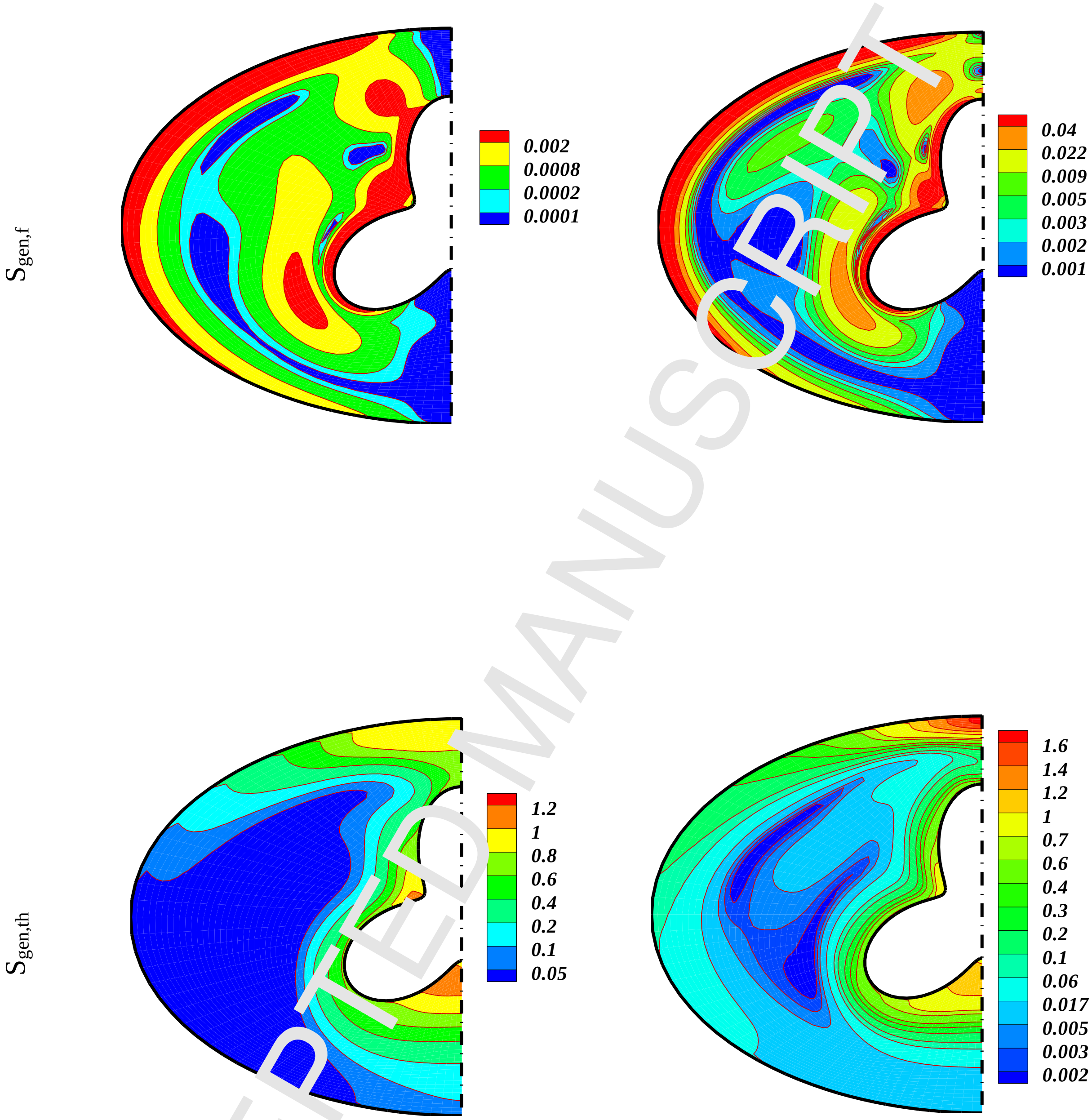
$S_{gen,f}$
0.002
0.0008
0.0002
0.0001
0.04
0.022
0.009
0.005
0.003
0.002
0.001
$S_{gen,th}$
1.2
1
0.8
0.6
0.4
0.2
0.1
0.05
1.6
1.4
1.2
1
0.7
0.6
0.4
0.3
0.2
0.1
0.06
0.017
0.005
0.003
0.002

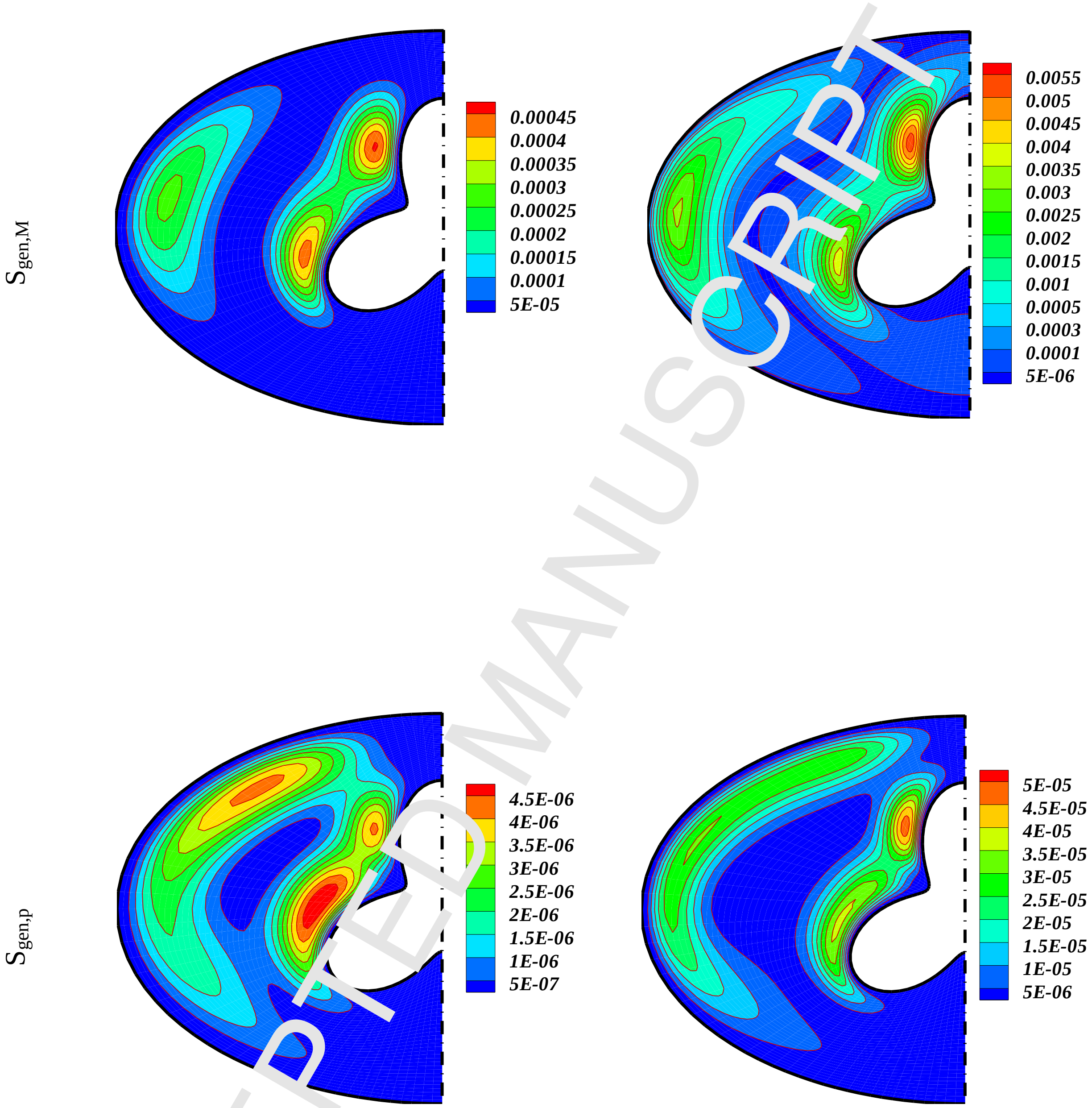
$S_{gen,M}$
0.00045
0.0004
0.00035
0.0003
0.00025
0.0002
0.00015
0.0001
5E-05
0.0055
0.005
0.0045
0.004
0.0035
0.003
0.0025
0.002
0.0015
0.001
0.0005
0.0003
0.0001
5E-06
$S_{gen,p}$
4.5E-06
4E-06
3.5E-06
3E-06
2.5E-06
2E-06
1.5E-06
1E-06
5E-07
5E-05
4.5E-05
4E-05
3.5E-05
3E-05
2.5E-05
2E-05
1.5E-05
1E-05
5E-06

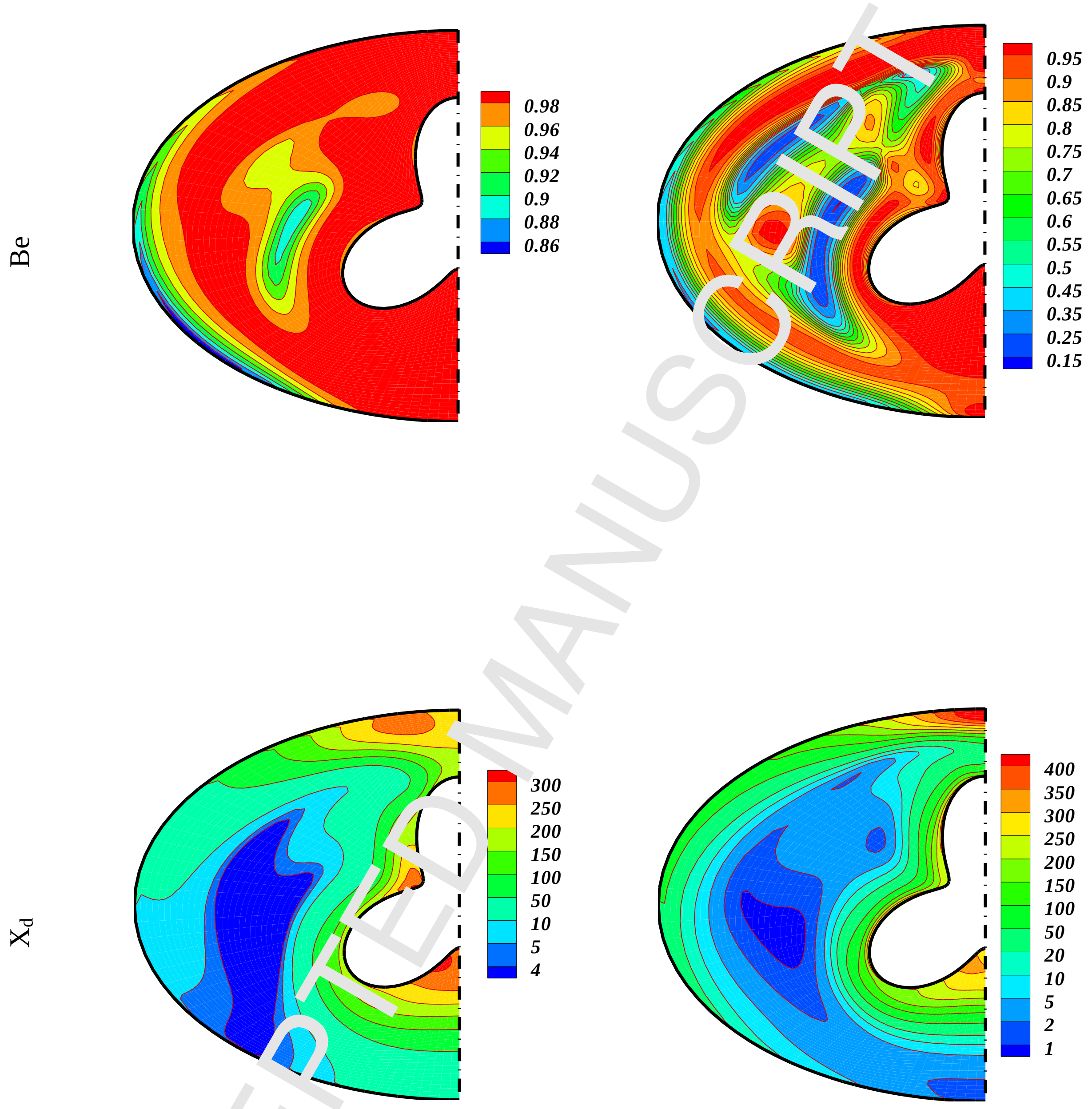

Fig. 4. Outputs for various Ra at $\phi = 0.04, Ha = 1, Da = 100$

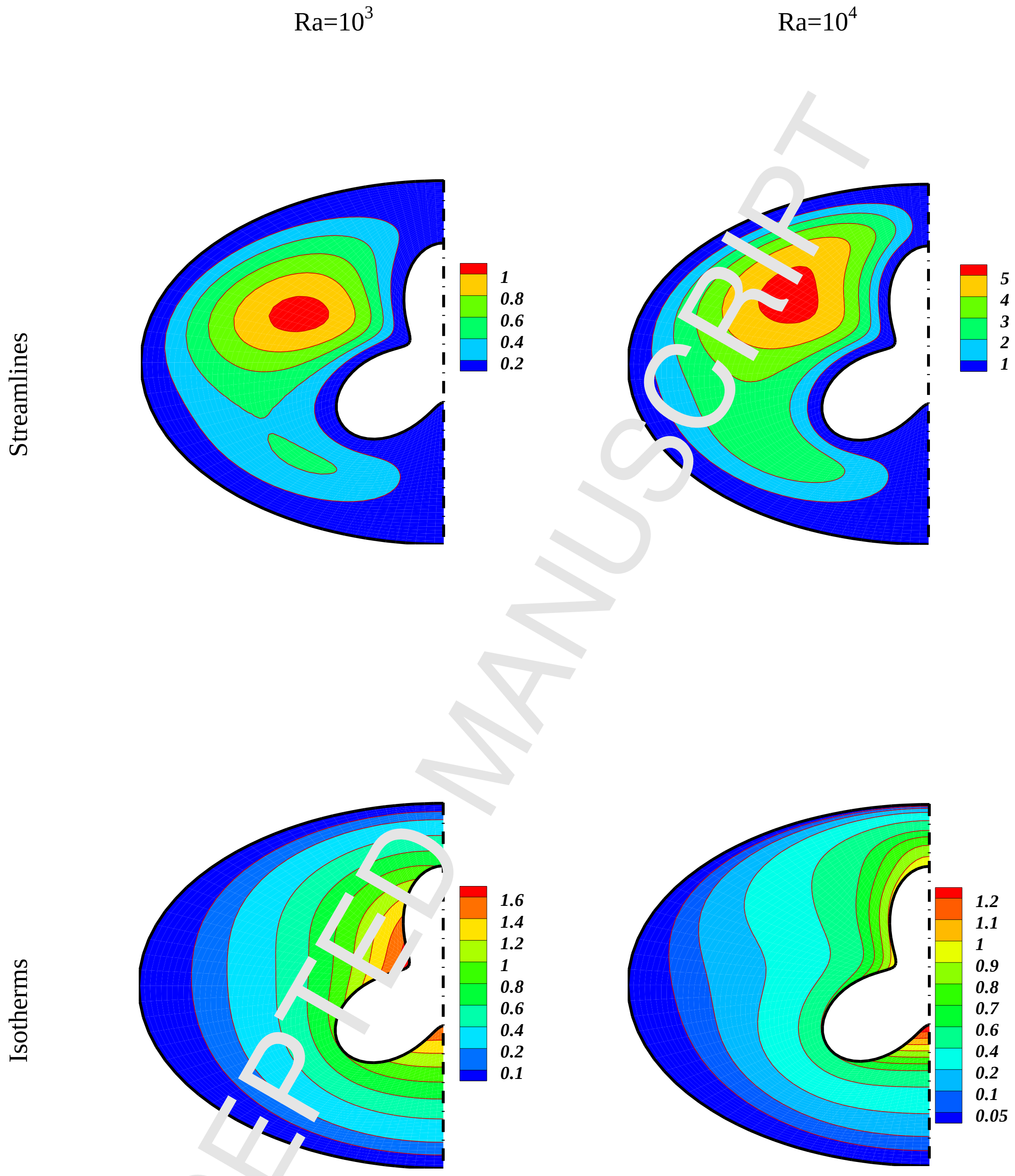
Ra=10^3
Ra=10^4
Streamlines
Isotherms
1
0.8
0.6
0.4
0.2
5
4
3
2
1
1.6
1.4
1.2
1
0.8
0.6
0.4
0.2
0.1
1.2
1.1
1
0.9
0.8
0.7
0.6
0.4
0.2
0.1
0.05

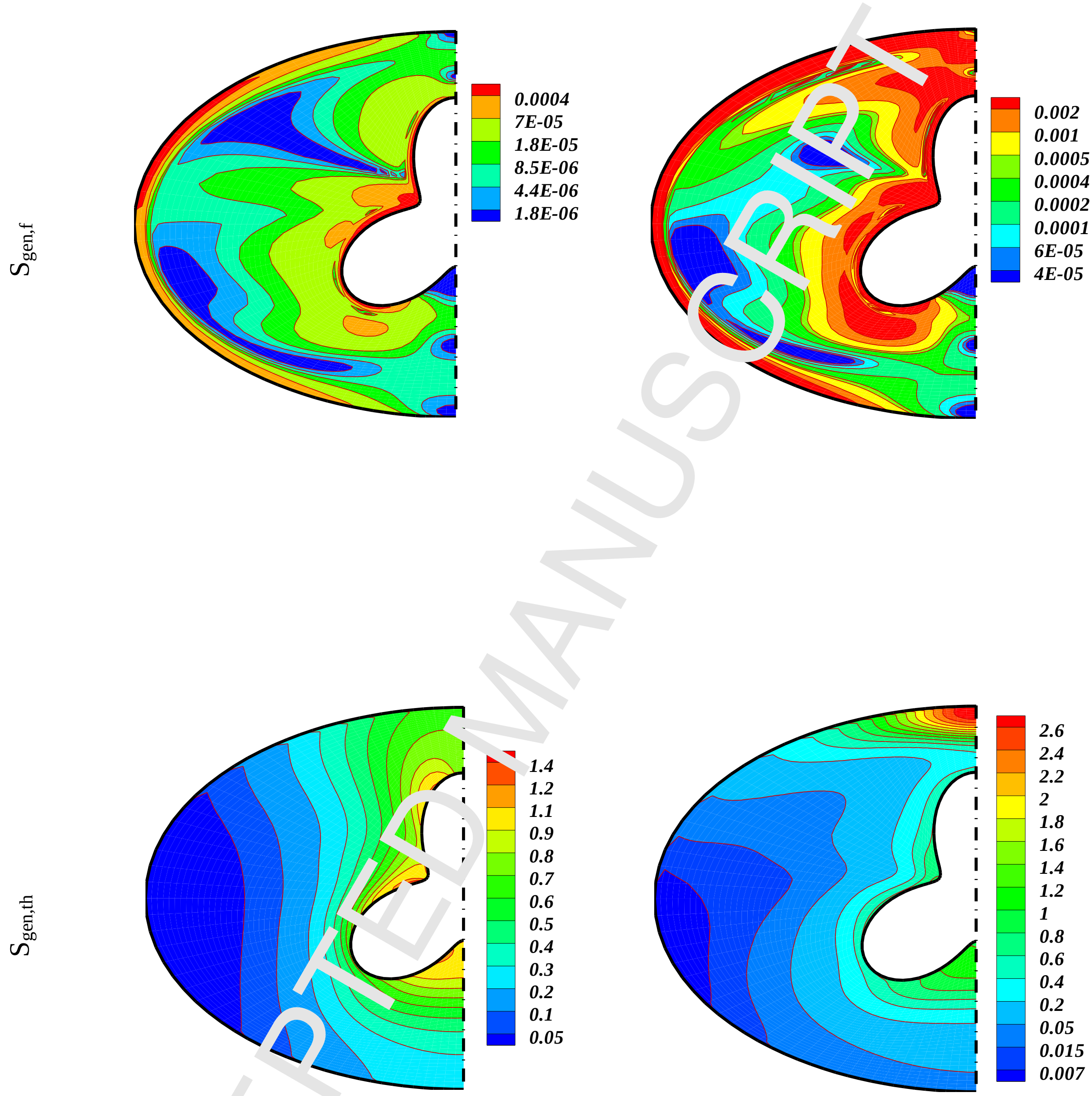
$S_{gen,f}$
0.0004
7E-05
1.8E-05
8.5E-06
4.4E-06
1.8E-06
0.002
0.001
0.0005
0.0004
0.0002
0.0001
6E-05
4E-05
$S_{gen,th}$
1.4
1.2
1.1
0.9
0.8
0.7
0.6
0.5
0.4
0.3
0.2
0.1
0.05
2.6
2.4
2.2
2
1.8
1.6
1.4
1.2
1
0.8
0.6
0.4
0.2
0.05
0.015
0.007

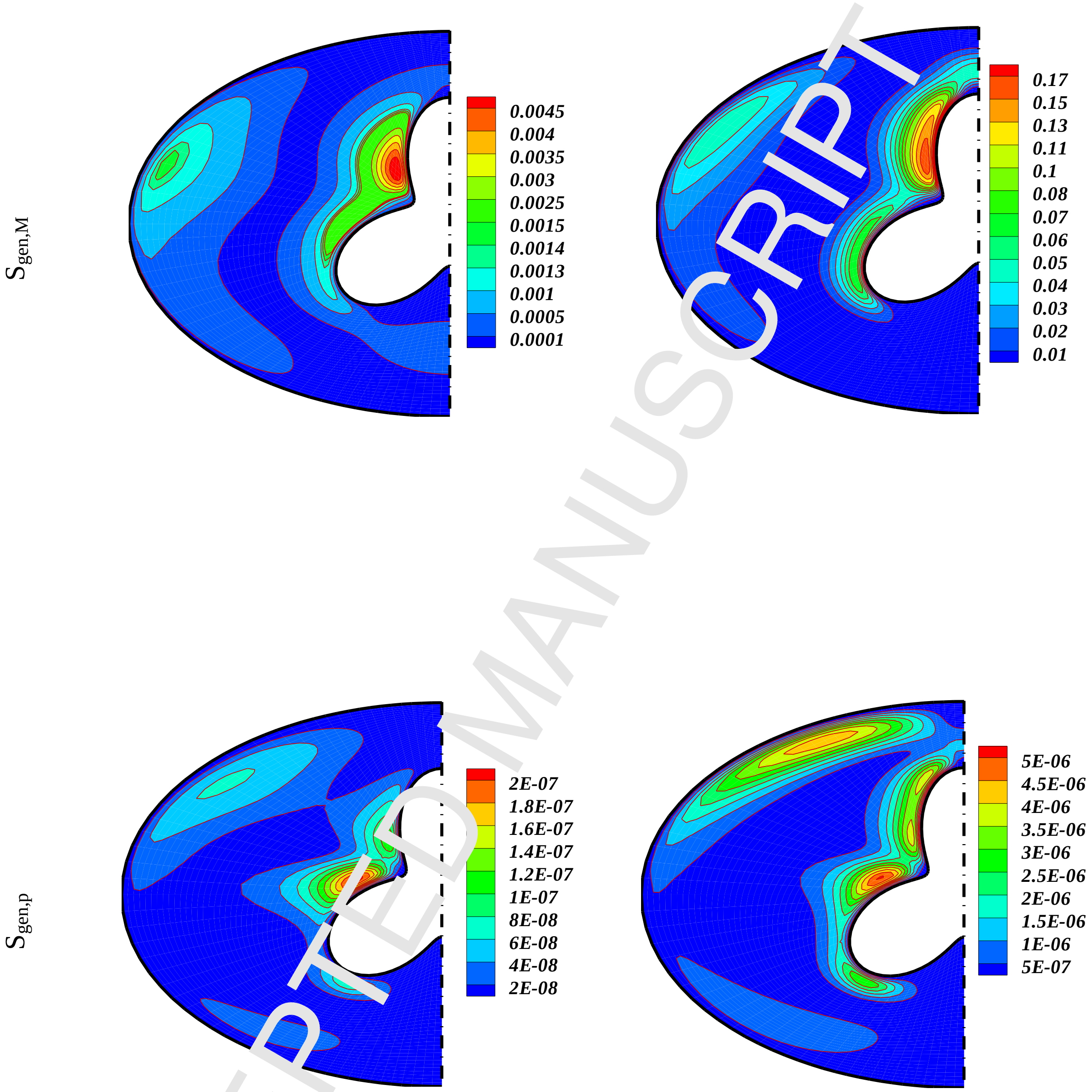

$S_{gen,M}$
0.0045
0.004
0.0035
0.003
0.0025
0.0015
0.0014
0.0013
0.001
0.0005
0.0001
0.17
0.15
0.13
0.11
0.1
0.08
0.07
0.06
0.05
0.04
0.03
0.02
0.01
$S_{gen,p}$
2E-07
1.8E-07
1.6E-07
1.4E-07
1.2E-07
1E-07
8E-08
6E-08
4E-08
2E-08
5E-06
4.5E-06
4E-06
3.5E-06
3E-06
2.5E-06
2E-06
1.5E-06
1E-06
5E-07

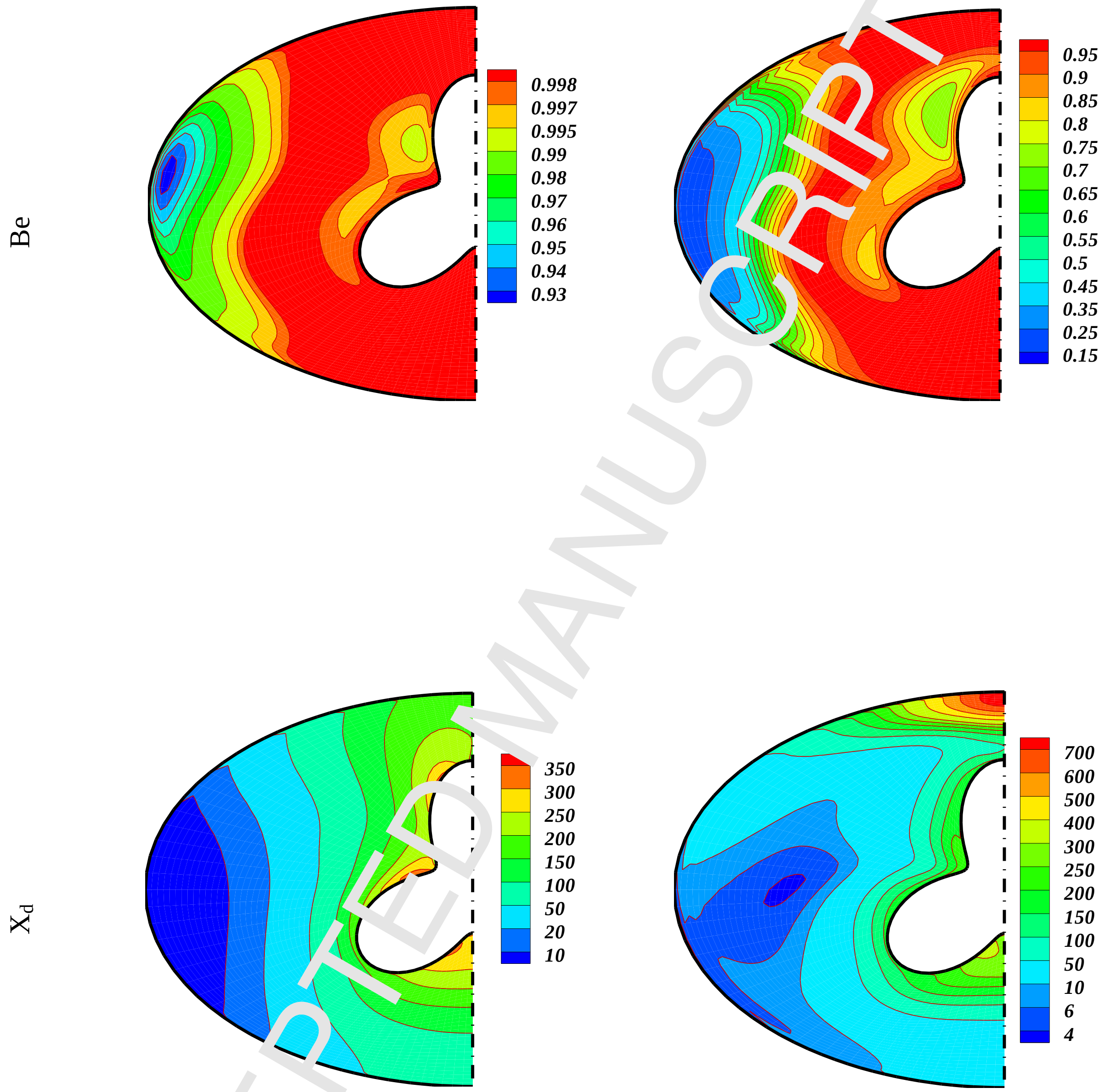

Fig. 5. Outputs for various Ra at $\phi = 0.04, Ha = 20, Da = 100$

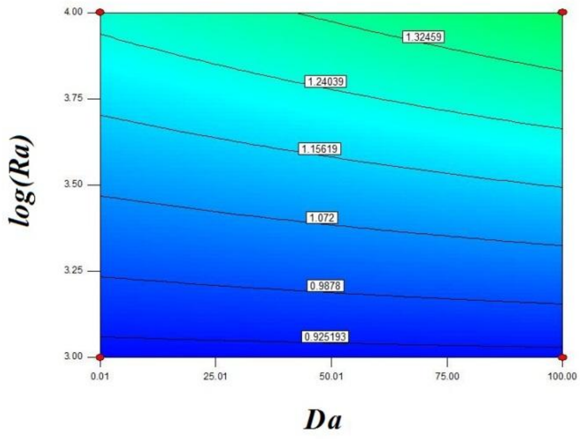

$Ha = 5$

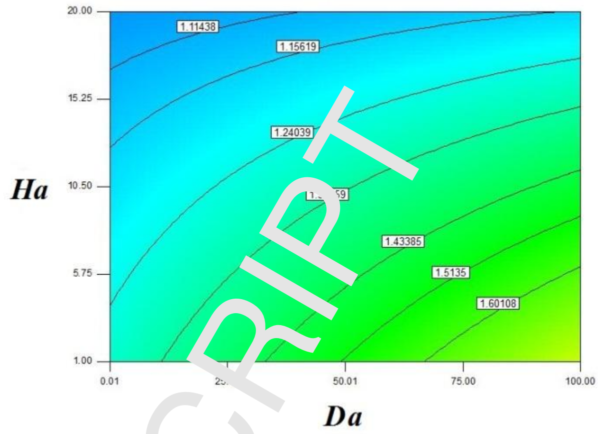

$\log(Ra) = 3.5$

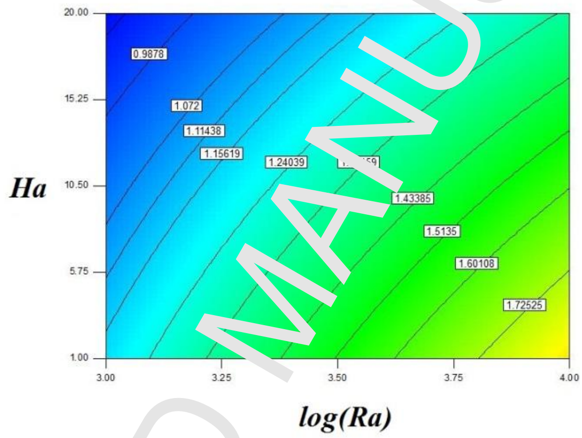

$Da = 50$

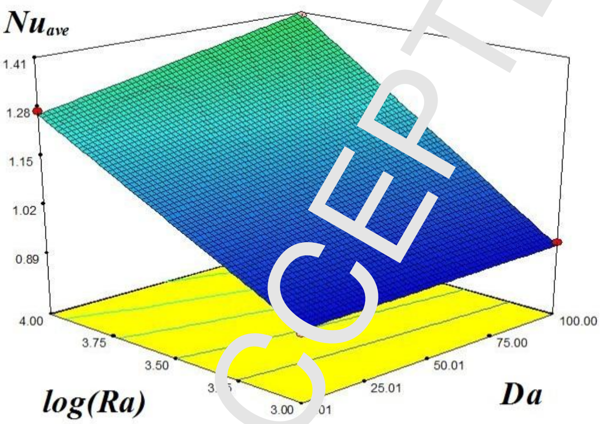

$Ha = 5$

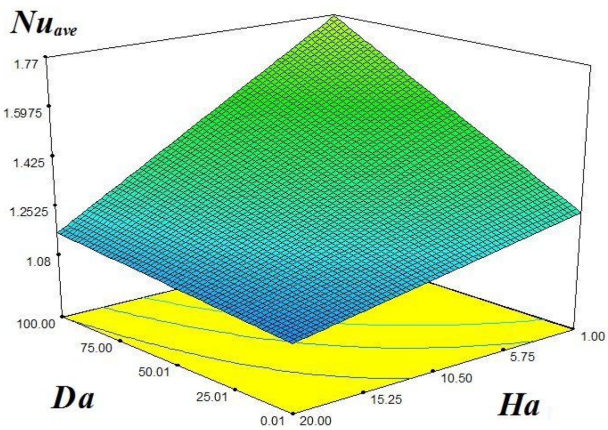

$\log(Ra) = 3.5$

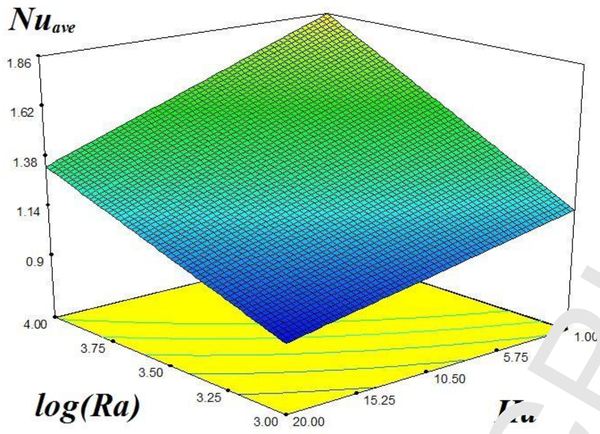

$Da = 50$

Fig. 6. Values of Nu_{ave} for various Ra, Ha, Da

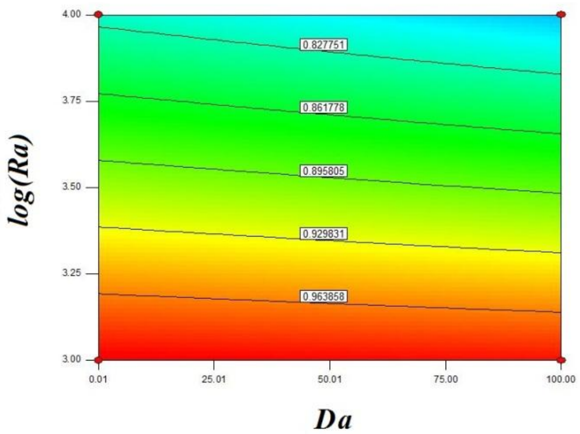

$Ha = 5$

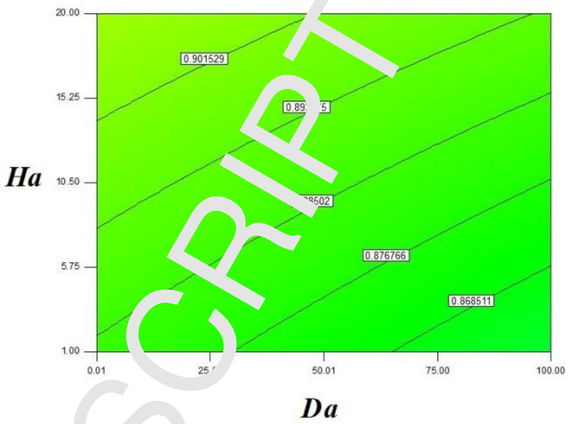

$\log(Ra) = 3.5$

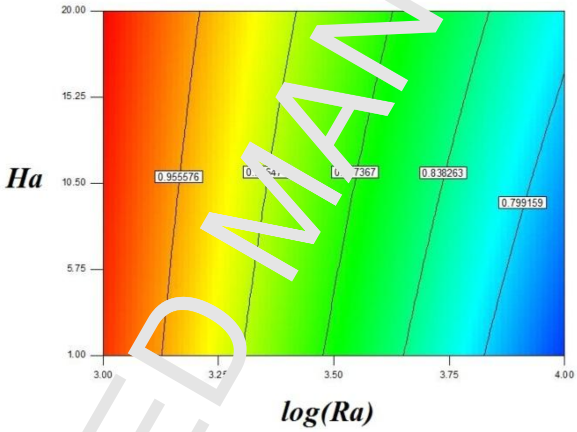

$Da = 50$

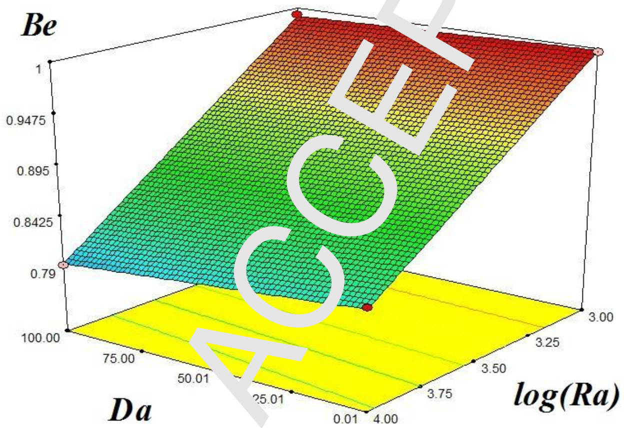

$Ha = 5$

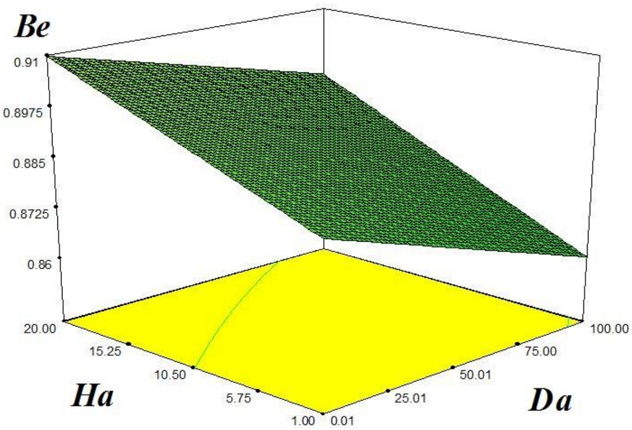

$\log(Ra) = 3.5$

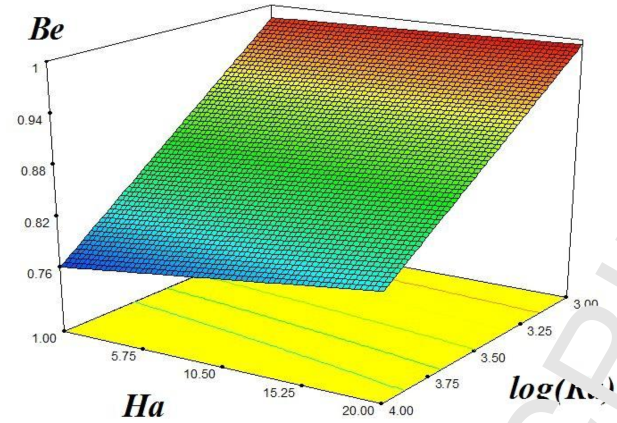

$Da = 50$

Fig. 7. Values of *Be* for various Ra, Ha, Da

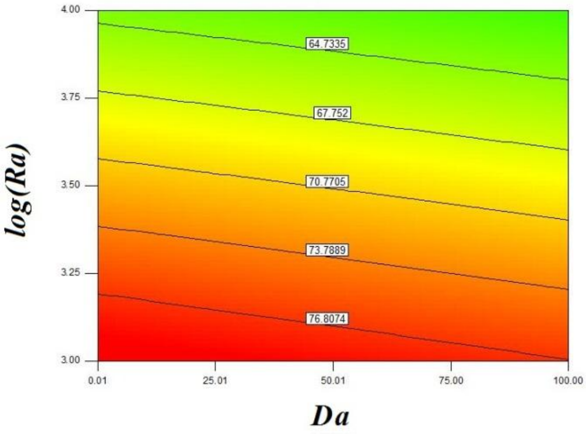

$Ha = 5$

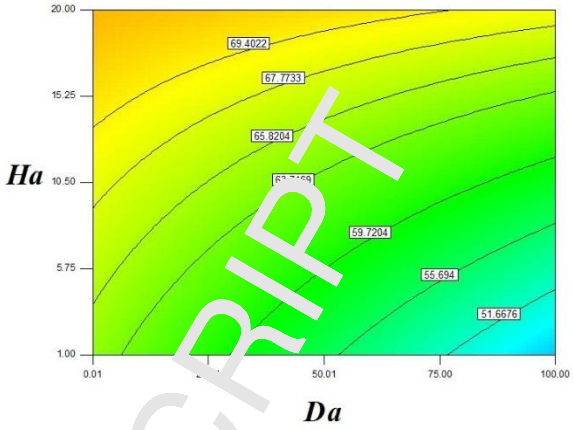

$\log(Ra) = 3.5$

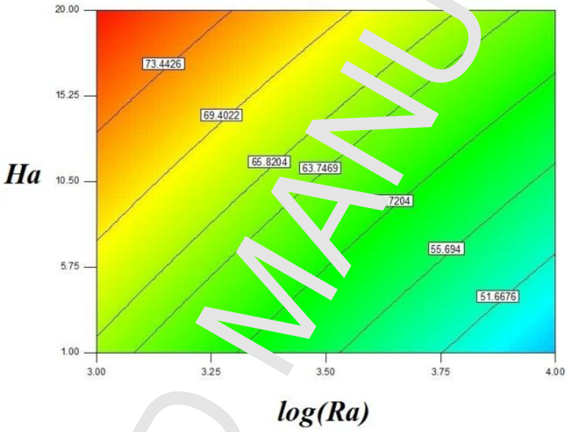

$Da = 50$

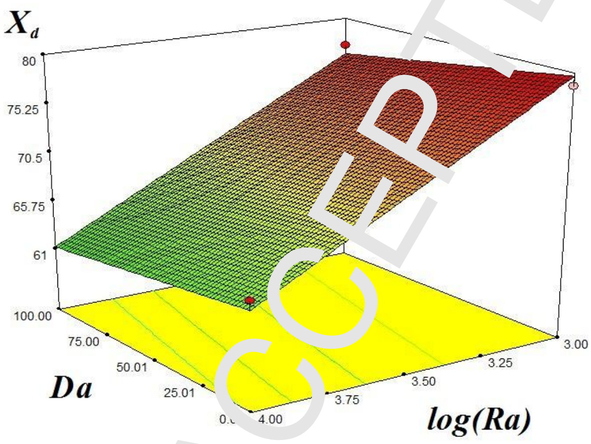

$Ha = 5$

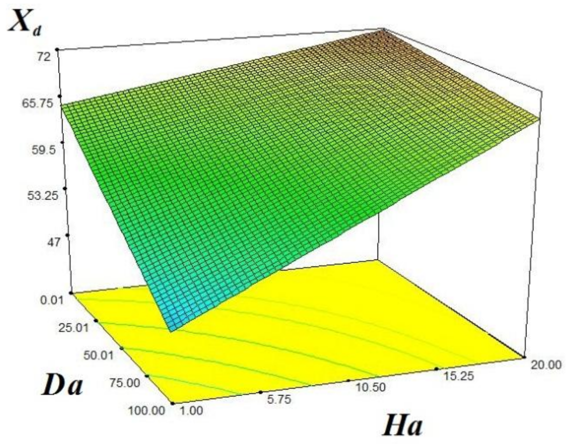

$\log(Ra) = 3.5$

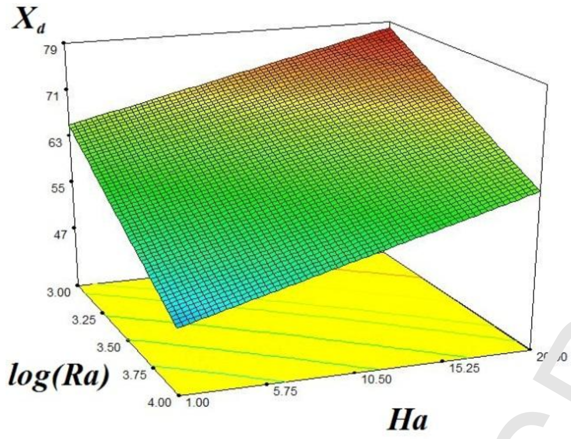

$Da = 50$

Fig. 8. Values of X_d for various Ra, Ha, Da

Table1. Features of H_2O and iron oxide

	Pure water	Fe_3O_4
$\sigma(\Omega \cdot m)^{-1}$	0.05	25000
$\beta \times 10^5 (K^{-1})$	21	1.3
$k(W/m.k)$	0.613	6
$C_p(j/kgk)$	4179	670
$\rho(kg/m^3)$	997.1	5200

Table2. Various grids and obtained Nu_{ave} at $Da = 100, Ha = 1, Ra = 10^4$ and $\phi = 0.04$.

51×151	71×211	
2.12102	2.15137	91×271
61×181	81×241	2.15804
2.14914	2.15365	

Table3. Comparison of current outputs with benchmark [30] at Pr=0.7.

	$Ra = 10^3$	$Ra = 10^4$	$Ra = 10^5$
De Vahl Davis [30]	1.118	2.243	4.519
Present	1.1432	2.2749	4.5199